Introduction

> I have gathered a posie of other men's flowers, and nothing but the thread that binds them is my own.
>
> Montaigne

Observational cosmology is in a tremendously exciting time of rapid discovery. Cosmology can be enriching and enjoyable at this level no matter what your aims are, but my guiding principle for the topics in this book has been: what would I ideally like a person finishing an undergraduate degree and starting a PhD in observational cosmology to know? What would represent a balanced undergraduate introduction that I would like them to have had?

Throughout this book, I've tried to give readers enough grounding to appreciate the current topics in this enormously active and exciting field, and to give some sense of the gaps — and in some cases chasms — in our understanding. I haven't forgotten that the step up to third-level undergraduate study can be difficult and daunting, so I've included further reading sections. Some of the items in these lists will take you to more leisured introductions and backgrounds to some of the material that we shall cover. Nevertheless, this book is intended to be fully self-contained.

I've also given some jumping-off points if readers want to go into more depth. You'll find these mostly in the further reading sections, but also in some footnotes and figure captions. There are some references to journal articles, such as 'Hughes et al., 1998, *Nature*, **394**, 241'. The first number is a volume number, and the second is a page number. Many of these can currently be read online, either in preprint form or as published papers, at http://adsabs.harvard.edu/abstract_service.html. Some of the further reading is most easily found on the internet, but internet addresses are transitory so I've tried to keep these to a minimum. References to arXiv or astro-ph reference numbers are to the preprint server, currently at http://arxiv.org or various worldwide mirrors. Entering the article identification in the search there usually results in the paper. Sometimes the further reading section will point to more advanced material, beyond the normal scope of an undergraduate degree. I've chosen to do this partly in order to ease the transition from undergraduate to postgraduate level for those of you who are on that track. The online abstract service also has the facility to list later papers that have cited any given paper, so it's very useful for literature reviews. At every stage, each level is a big step up from the previous one and the transition can be difficult. I don't intend this book to be a postgraduate textbook, but if I can ease the transition to that level, then all to the good.

Inevitably the selection of topics betrays my own biases and interests, and there are undoubtedly many exciting areas not covered. But the biggest problem is that this is a fast-paced field with lots of exciting and rapid developments. Some future advances are foreseeable, such as gravitational wave astronomy or the Square Kilometre Array, and I can give tasters for what these fabulous new facilities promise, so this book should keep its relevance for a few years at least. As I write this, the Herschel and Planck satellites are waiting to be launched in French Guyana. However, the 'unknown unknowns' I can do nothing about. This is the mixed blessing of writing a book during the golden age of cosmology.

Finally, I would like to thank David Broadhurst, Mattia Negrello, Andrew Norton, Robert Lambourne, Jim Hague and Carolyn Crawford for their critical readings of early drafts of this book. Any errors that I somehow managed to sneak through their careful ministrations are down to me alone. I would also like to thank the editors and artists at The Open University for turning my scribbles into something beautiful.

Chapter 1 Space and time

God does not care about our mathematical difficulties. He integrates empirically.

Albert Einstein

Introduction

How did the Universe begin? How big is the observable Universe? Why is the night sky dark? What will the Universe be like in the year one trillion? What is the ultimate fate of the Universe? This chapter will answer these questions and more, and give you the tools that you need for understanding modern precision cosmology.

Although it's not necessary for you to have met special relativity and the Robertson–Walker metric before, you may find that we take these subjects at a fast pace in this chapter if these are new topics to you. If so, you may find Appendix B on special relativity helpful, or you might try a more comprehensive introduction to expanding spacetime metrics such as that in Robert Lambourne's *Relativity, Gravitation and Cosmology* (see the further reading section).

1.1 Olbers' paradox

In 1823, the Dutch astronomer Heinrich Wilhelm Olbers asked a profound question: if the Universe is infinite, then every line of sight should end on a star, so why isn't the night sky as bright as the Sun? The fact that these stars are further away doesn't help, as we'll show.

At a distance r from the Sun, its light is spread evenly over a sphere with an area $4\pi r^2$, as shown in Figure 1.1. If the Sun has luminosity L, then the energy flux S from the Sun must be

$$S = \frac{L}{4\pi r^2}, \tag{1.1}$$

i.e. $S \propto L/r^2$. Meanwhile, if the diameter of the Sun is D, then the angular diameter θ of the Sun (see Figure 1.2) will be given by

$$\theta \simeq \tan\theta = \frac{D}{r},$$

where the approximation $\theta \simeq \tan\theta$ is valid for small angles measured in radians. Therefore we have

$$\theta \propto \frac{D}{r}.$$

So the Sun's angular area on the sky (in, for example, square degrees or steradians) must be proportional to $(D/r)^2$. Therefore the **surface brightness** (flux per unit area on the sky, e.g. per square degree) is proportional to $(L/r^2)/(D/r)^2 = L/D^2$, which is a constant independent of r. So if all stars are like the Sun (i.e. similar luminosities and diameters), then all stars should have surface brightnesses similar to that of the Sun. If every line of sight ends on a star, then the whole sky should be about as bright as the Sun.

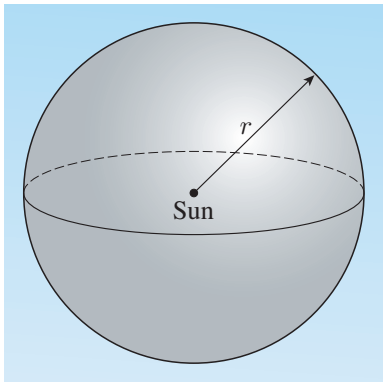

Figure 1.1 A sphere of radius r surrounding the Sun.

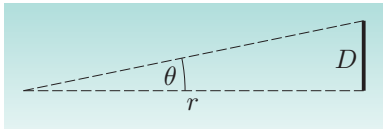

Figure 1.2 The angle θ varies approximately as D/r.

1.2 Olbers' paradox in a different way

Here is a different approach to the same problem. Suppose that there are ρ stars per unit volume, in a Universe that's homogeneous (the same seen from every point) and isotropic (no preferred direction). How many stars have fluxes in the range S to $S + \mathrm{d}S$? (Here, $\mathrm{d}S$ can be thought of as a limitingly-small[1] increment of S, which we use in preference to δS.) First, let's assume for now that all stars are identical, and have luminosity L. Consider a radial shell around the Earth, with radius r and thickness $\mathrm{d}r$ (Figure 1.3). The volume of this shell is the area times the thickness, or $4\pi r^2\,\mathrm{d}r$. (Another way of finding the volume of the shell is to subtract $\frac{4}{3}\pi r^3$ from $\frac{4}{3}\pi(r+\mathrm{d}r)^3$, and neglect terms of the order $(\mathrm{d}r)^2$.) The number of stars in this shell is ρ times the volume of the shell:

$$\mathrm{d}N = \rho \times 4\pi r^2\,\mathrm{d}r \propto \rho r^2\,\mathrm{d}r. \tag{1.2}$$

(We're assuming a flat space for now, known as **Euclidean** space — curved spaces will come later.) The flux S of a star varies with distance according to Equation 1.1, which implies that

$$\frac{\mathrm{d}S}{\mathrm{d}r} \propto Lr^{-3}.$$

So the number of stars with fluxes between S and $S + \mathrm{d}S$ is

$$\mathrm{d}N = \frac{\mathrm{d}N}{\mathrm{d}S}\,\mathrm{d}S = \frac{\mathrm{d}N}{\mathrm{d}r}\,\frac{\mathrm{d}r}{\mathrm{d}S}\,\mathrm{d}S$$
$$\propto \rho r^2 \frac{r^3}{L}\,\mathrm{d}S \propto r^5\,\mathrm{d}S. \tag{1.3}$$

This $\mathrm{d}N$ is the same as in Equation 1.2; all stars have the same luminosity L, so Equation 1.1 gives an exact one-to-one correspondence between S and r, so the interval $(r, r+\mathrm{d}r)$ corresponds exactly to an interval $(S, S+\mathrm{d}S)$.

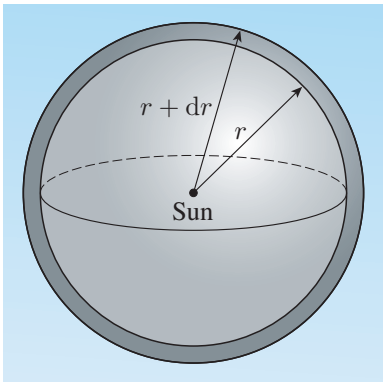

Figure 1.3 A shell of radius r and thickness $\mathrm{d}r$ around the Sun.

We can also write the last result as $\mathrm{d}N/\mathrm{d}S \propto r^5$. Now, by rearranging Equation 1.1 we have that

$$r = \left(\frac{L}{4\pi S}\right)^{1/2} \propto S^{-1/2}$$

and therefore

$$\frac{\mathrm{d}N}{\mathrm{d}S}\,\mathrm{d}S \propto S^{-5/2}\,\mathrm{d}S.$$

So we find that

$$\frac{\mathrm{d}N}{\mathrm{d}S} \propto S^{-5/2}. \tag{1.4}$$

Relations of this kind are known in cosmology as **number counts** or **source counts**, and play an important role, as we'll see. $\mathrm{d}N/\mathrm{d}S$ is the number of stars $\mathrm{d}N$ in a flux interval $\mathrm{d}S$, which is a slightly different way of regarding the rate of increase of N with respect to S. The general form $y \propto x^a$ is sometimes

[1] The infinitesimal quantity $\mathrm{d}S$, which we refer to vaguely as a 'limitingly-small' version of δS, can be defined more rigorously using a mathematical discipline called *non-standard analysis*. This takes us beyond the scope of this book, but if you are concerned by manipulating infinitesimals no differently to other algebraic symbols, try, for example, H. Jerome Keisler's book *Elementary Calculus: An Approach Using Infinitesimals*, which is available online.

called a **power law**, with a in this case being the **power law index**. Here, $\mathrm{d}N/\mathrm{d}S$ is a power law function of S, with a power law index of $-5/2$.

Now, we've assumed that all the stars are identical, but suppose instead that there are several types of star, each with a different luminosity L_i and number density ρ_i, with $i = 1, 2, 3, \ldots$. Each type of star will have its own number counts $\mathrm{d}N_i/\mathrm{d}S = k_i S^{-5/2}$, where k_i is some constant specific to type i. The total number counts will still obey a $-5/2$ power law:

$$\frac{\mathrm{d}N}{\mathrm{d}S} = \sum \frac{\mathrm{d}N_i}{\mathrm{d}S} = \sum \left(k_i S^{-5/2} \right) = S^{-5/2} \sum k_i \propto S^{-5/2}.$$

So any homogeneous, isotropic population of stars produces a $-5/2$ power law for number counts. But this leads to a profound problem: the total flux of stars brighter than S_0 is

$$S_{\text{total}} = \int_{S_0}^{\infty} S \frac{\mathrm{d}N}{\mathrm{d}S} \, \mathrm{d}S \propto \int_{S_0}^{\infty} S^{-3/2} \, \mathrm{d}S \propto S_0^{-1/2},$$

which diverges as S_0 tends to zero. So the sky should be infinitely bright!

Exercise 1.1 First, we've argued that a homogeneous, isotropic Universe gives you a sky as bright as the Sun. Next, we've argued that the sky is infinitely bright in a homogeneous, isotropic Universe. They can't both be true, and it's not a mistake in the algebra, so what's different in our assumptions? ■

The night sky is a long way from being as bright as the Sun, and is certainly not infinitely bright. So what is the answer to Olbers' profound question? It's not that the Universe is opaque — in fact, as we shall see later in this book, the Universe is surprisingly transparent at optical wavelengths. It's also not that stars have finite lifetimes, because that doesn't stop lines of sight ending on a star eventually and inevitably.

Part of the answer is that the Universe is only finitely old. Edgar Allan Poe was the first to point out this solution, in his 1848 book *Eureka: a Prose Poem*. But another part of the answer is that we don't live in a static, flat space. Rather, we live in a curved, expanding spacetime, which we shall meet in the next section.

1.3 Metrics: the Universe in a nutshell

We're about to commit possibly the greatest ever act of hubris: to describe the geometry of the Universe in a single equation. To do this, we'll need to remind you of a few preliminaries and notations. Pythagoras's theorem is

$$H^2 = x^2 + y^2$$

for a right-angled triangle with length x, height y and hypotenuse H. In three dimensions this is just

$$H^2 = x^2 + y^2 + z^2.$$

So, if two points in space are separated by $(\delta x, \delta y, \delta z)$, their separation δL is given by

$$(\delta L)^2 = (\delta x)^2 + (\delta y)^2 + (\delta z)^2.$$

In pre-relativistic physics, if one observer measures the separation to be δL, then all observers measure the same δL regardless of how they are moving. This also has all observers agreeing over the passage of time: a separation in time of δt of two events is the same for all observers. (**Event** is used to mean a point in *both* space and time.) The whole aim of fundamental physics is to describe the workings of the Universe in an observer-independent way, so these observer-independent quantities, called **invariants**, often play a central role. This is why it's meaningless to say that the laws of physics are different somewhere else in the Universe: if they're different somewhere else, they weren't fundamental laws in the first place. Many quantities in physics owe almost all their interest to the fact that they are conserved in all (or nearly all) situations: energy, momentum, angular momentum, baryon number, lepton number, strangeness, isospin.

Having said that, there is currently no consistent theory of everything. The best description of the very small, quantum physics, contradicts the best theory of the very large, general relativity. We proceed in the hope that the apparently-invariant quantities discovered so far will lead us closer to the underlying workings of the Universe ...

In Einstein's special relativity, neither spatial separations nor time intervals are invariant, but there is a combined spacetime interval that *is* invariant:

$$(\delta s)^2 = (c\,\delta t)^2 - (\delta x)^2 - (\delta y)^2 - (\delta z)^2, \tag{1.5}$$

where c is the speed of light in a vacuum. The coefficients on the right-hand side (in this case $+1, -1, -1, -1$) are known as the **metric coefficients**. (Note that some books choose to use a $(-1, 1, 1, 1)$ metric instead.) Together, these coefficients make up the **metric tensor** (see Appendix B); we shall discuss tensors later in this book.

The metric of special relativity has many consequences with which you should be familiar, such as time dilation, Lorentz contraction, Lorentz transformations and the non-universality of simultaneity. If you need reminders, Appendix B gives a very brief summary of special relativity. Freely falling particles move on paths for which the total interval s is a maximum along that path, similarly to Fermat's principle in optics. These optimal paths are known as **geodesics**.

Worked Example 1.1

Two ticks of a watch are separated by $(\delta t, 0, 0, 0)$ in the frame of the watch, with $\delta t = 1$ second. The watch is moving at a constant velocity v relative to an observer, for whom the ticks are separated by $(\delta t', \delta x', \delta y', \delta z')$. Using Equation 1.5 or otherwise, show that $\delta t' = \gamma(v)\,\delta t$ with $\gamma = (1 - v^2/c^2)^{-1/2}$, and calculate the spacetime interval δs between the ticks.

If I put the watch on a piece of string and whirl it around my head, and it takes half a second (according to the watch) to go round once, what is the total spacetime interval of the watch's world-line of one orbit? (A world-line is the set of events that trace the path of an object through spacetime.)

Solution

Without loss of generality, we can choose coordinates in which the observer is moving along the x-axis, so $\delta y' = \delta z' = 0$. Now $v = \mathrm{d}x'/\mathrm{d}t'$, and from $\delta s' = \delta s$ we have $(c\,\delta t)^2 = (c\,\delta t')^2 - (\delta x')^2$. If we divide by $(c\,\delta t')^2$, we find

$$\frac{c^2(\delta t)^2}{c^2(\delta t')^2} = 1 - \frac{(\delta x')^2}{c^2(\delta t')^2} = 1 - \frac{(\mathrm{d}x')^2}{c^2(\mathrm{d}t')^2},$$

so

$$\left(\frac{\delta t}{\delta t'}\right)^2 = 1 - \left(\frac{\mathrm{d}x'}{c\,\mathrm{d}t'}\right)^2 = 1 - \frac{v^2}{c^2}$$

hence

$$\delta t' = \gamma(v)\,\delta t.$$

For the second part, $\delta s = c\,\delta\tau$, where τ is the proper time, i.e. the time measured by the watch. Here, we have $\delta\tau = \delta t$, so the total interval is $0.5c$ metres, or 0.5 light-seconds. When the watch is being whirled around, τ is in an accelerating frame, but *it's always true that* $\delta s = c\,\delta\tau$, so the total interval is 0.5 light-seconds.

Worked Example 1.2

What is the total spacetime interval between any two points on a light ray, and how does the interval relate to causality in the Universe? (*Hint*: If events can be connected only by a signal travelling faster than light, they cannot be in causal contact with each other.)

Solution

The spacetime interval between any two points on a light ray is zero. The connection to causality is best illustrated in the lightcone diagram shown in Figure 1.4. An event at the origin can send a message at light speed or slower to any event in the future lightcone. Similarly, any event in its past lightcone could have affected it. The spacetime intervals between the origin and these events are **time-like** intervals, $(\delta s)^2 > 0$. Events outside the lightcone cannot affect, or be affected by, the event at the origin. The spacetime intervals between the origin and these events are **space-like**, i.e. $(\delta s)^2 < 0$. Points on the lightcone have exactly zero spacetime interval between one another. The $\delta s = 0$ intervals are sometimes referred to as **null**.

Exercise 1.2 The highest-energy cosmic rays have energies of 10^{20} eV and above. Most cosmic rays are protons, with rest masses of $938.28\,\mathrm{MeV}/c^2$. The diameter of our Galaxy is roughly 100 000 light-years. Calculate how long it would take to cross the Galaxy, according to the highest-energy cosmic rays. (*Hint*: You don't need to know the conversion between eV and joules, nor do you need the conversion between light-years and metres.) ■

We can also describe the invariant spacetime interval in spherical coordinates, in infinitesimals:

$$\mathrm{d}s^2 = (c\,\mathrm{d}t)^2 - \mathrm{d}r^2 - (r\,\mathrm{d}\theta)^2 - (r\sin\theta\,\mathrm{d}\phi)^2,$$

where $\mathrm{d}s^2$ means $(\mathrm{d}s)^2$. These coordinates are shown in Figure 1.5.

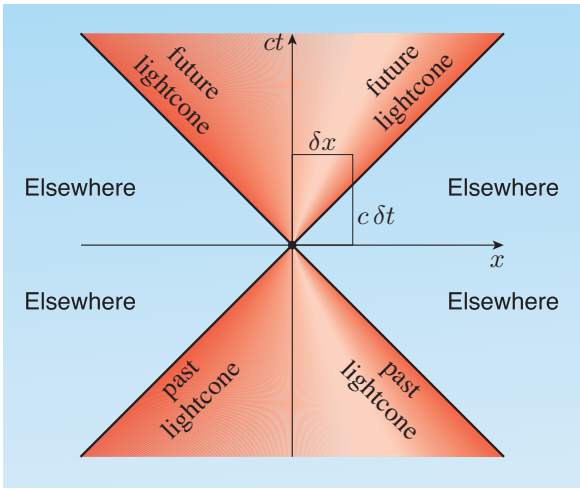

Figure 1.4 The lightcone in special relativity. The point at position $(\delta x, c\,\delta t)$ has $c\,\delta t > \delta x$, so $(c\,\delta t)^2 - (\delta x)^2 > 0$, implying that $(\delta s)^2 > 0$, meaning that the invariant interval between that point and the origin is time-like.

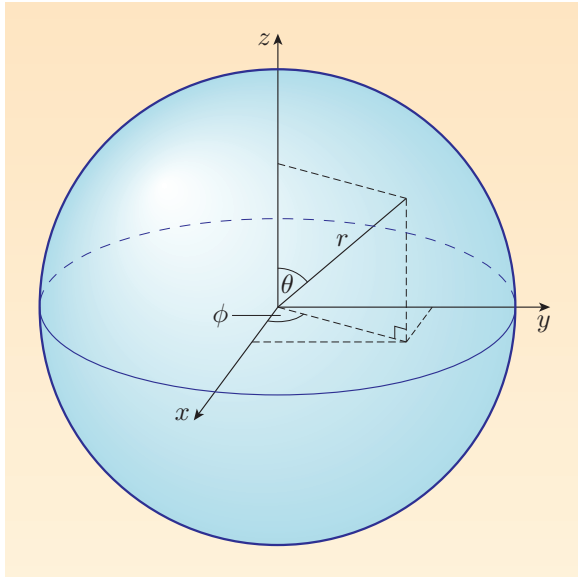

Figure 1.5 The position of a point can be specified in terms of Cartesian coordinates (x, y, z) or in terms of spherical coordinates (r, θ, ϕ).

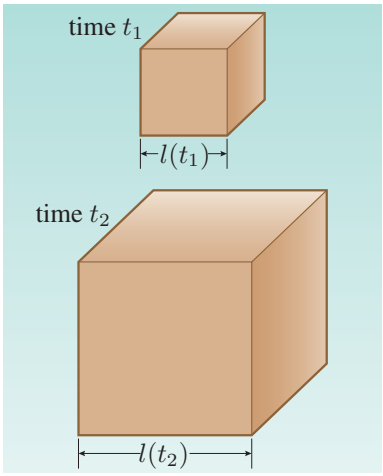

Figure 1.6 A cubical volume of the Universe. The length of the side l expands with the scale factor of the Universe, so $l(t_2) = (R(t_2)/R(t_1))\,l(t_1)$.

To describe an expanding Universe, we could modify the metric by multiplying the spatial parts with a time-dependent expansion factor:

$$\mathrm{d}s^2 = c^2\,\mathrm{d}t^2 - R(t)\left(\mathrm{d}r^2 + r^2\,\mathrm{d}\theta^2 + r^2\sin^2\theta\,\mathrm{d}\phi^2\right),$$

where $R(t)$ is called the **scale factor** of the Universe. A schematic representation of this is shown in Figure 1.6.

In fact, the most general homogeneous, isotropic metric is

$$\mathrm{d}s^2 = c^2\,\mathrm{d}t^2 - R^2(t)\left(\frac{\mathrm{d}r^2}{1-kr^2} + r^2\,\mathrm{d}\theta^2 + r^2\sin^2\theta\,\mathrm{d}\phi^2\right), \qquad (1.6)$$

where the constant k determines whether the Universe is spatially flat ($k = 0$), spherical ($k = +1$) or hyperbolic ($k = -1$). (We use only these three values of k because other values can be found by rescaling R and r; for example, if $k = -3$, then the substitutions $r' = r\sqrt{3}$ and $R' = R/\sqrt{3}$ give an equation of the same form as Equation 1.6 for $k = -1$.) Figure 1.7 illustrates some two-dimensional surfaces in which $k = +1$, 0 or -1, to give you some intuition (if not actually a visualization) of the three-dimensional counterparts. You might reasonably object that these two-dimensional representations oversimplify the situation. In physics (and general relativity especially) it's often easier to describe something mathematically than it is to visualize it; physics makes tremendous demands on

the imagination. Perhaps the human brain doesn't have the cognitive machinery to be able to visualize curved expanding spacetimes.

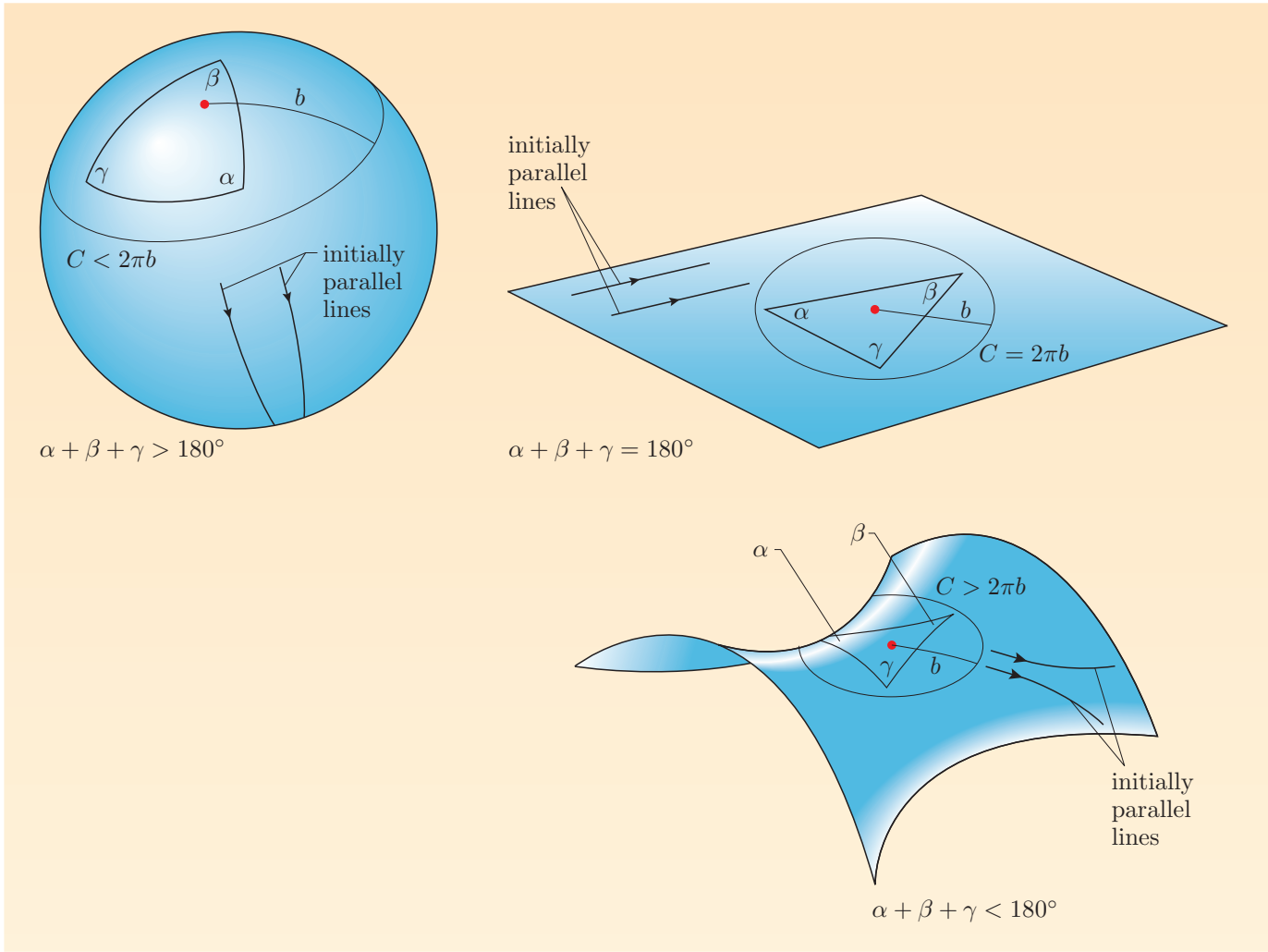

Figure 1.7 Curved surfaces may have geodesics that start parallel, but don't remain parallel. Also, the angles of a triangle need not add up to 180°, nor is the circumference of a circle necessarily 2π times the radius. The spherical model has $k = +1$, the flat model has $k = 0$ and the saddle-shaped model has $k = -1$.

Equation 1.6 is known as the **Robertson–Walker metric** or sometimes as the **Friedmann–Robertson–Walker metric**. Because this metric is spatially homogeneous and isotropic, any point can be chosen for the origin $r = 0$. We sometimes refer to t as coordinate time or **cosmic time**. This metric has preferred inertial reference frames in which the expansion of the Universe is isotropic. It's in such a frame that the coordinates t, r, θ, ϕ are measured. We'll refer to this reference frame as the **cosmic rest frame**, and it's assumed to be equivalent to the frame of the cosmic microwave background, of which more later. If we took an observer in the cosmic rest frame and applied a velocity boost (a Lorentz transformation) to see what the expanding Universe would look like from a moving observer's point of view, we'd find that it no longer looked isotropic.

Equation 1.6 is our hubristic attempt to describe the Universe in one line, and we shall meet this equation many times in this book.

It may now be worth discussing some frequent misconceptions about the Robertson–Walker metric.

- If the Universe is expanding, why am I not getting taller?
- Your head is not free-floating from your feet; your body is bound by chemical bonds.
- Why does the Earth not drift away from the Sun as the Universe expands?
- Equation 1.6 describes a Universe that is exactly homogeneous and isotropic. Locally, though, that's obviously not right. Within the Solar System the local metric is not the Robertson–Walker metric, because the gravitational field of the Sun dominates. Equation 1.6 is an approximation that becomes increasingly good at larger and larger scales, but on small scales spacetime clearly has much more structure. When we consider the collapse of density perturbations in Chapter 4, we'll see that it's wrong to think of the Earth feeling a gentle tug from the expansion of the Universe, which is overwhelmed by the attraction from the Sun.
- What is the Universe expanding into?
- In general relativity, the intrinsic curvature of spacetime (including the expansion of space) can be specified using measurements *within* the spacetime, using geodesics. This means that if we want to describe the curvature of spacetime, we don't need to embed spacetime in a higher-dimensional space. But if we don't need to refer to higher-dimensional space, and it doesn't affect anything that we can measure, do we need to hypothesize its existence at all? In any case, we would have no reason to believe that this higher-dimensional space is flat anyway. So, we don't have evidence that the Universe is expanding 'into' anything at all — it is simply expanding.
- Where is the middle of the Universe, which everything exploded out of?
- This is a widely-held misconception that perhaps dates back to Lemaître's phrase 'the primeval atom'. We frequently illustrate the expansion of space with an analogy of an expanding balloon (such as in Figure 1.8), but what is rarely pointed out is that the radial coordinate is *time-like*, not space-like. The explosion started at the centre, but this was at the beginning of *time* in the Robertson–Walker universe, not in a particular location. In fact, one might reasonably say that it occurred everywhere, at every point in space. Also, if the Universe is hyperbolic ($k = -1$), then the Universe may be infinite. If so, then even in the earliest moments of the history of the Universe, there would still be infinitely more matter outside any given volume than inside that volume.
- What caused the Universe to fling itself apart in the Big Bang?
- This question suggests an input of energy, flinging matter from an initial state of rest, but this is not how the field equations of general relativity are formulated. Classically at least, the answer is that these are just the initial conditions to Einstein's field equations. But just saying 'that's how it started' is clearly a very unsatisfactory answer, and arguably avoiding the question. One attraction of the theory of inflation is that it gives a mechanism for this initial expansion; we shall meet inflation in later chapters.

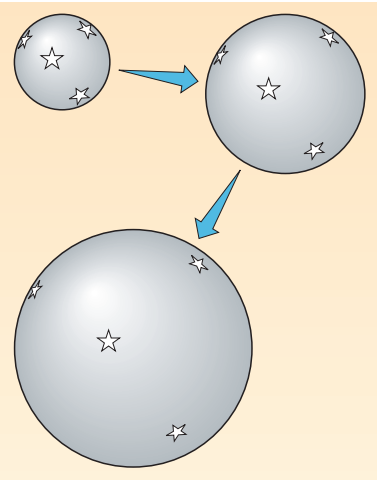

Figure 1.8 The balloon metaphor for the expanding Universe. Note that the objects on the balloon don't themselves expand.

Note that Equation 1.6 defines a preferred reference frame, in which the expansion is isotropic. As we shall see, this is well-supported by observations both of the large-scale structure of the galaxy distribution, and of the cosmic microwave background. Nevertheless, is it possible to conceive of a universe consistent with Einstein's field equations in which there are no preferred reference frames? One possibility is a fractal structure, and we shall meet this in later chapters when discussing inflation.

The field equations of Einstein's general relativity determine both k and $R(t)$. These equations can be shown to yield

$$\left(\frac{\mathrm{d}R}{\mathrm{d}t}\right)^2 = \dot{R}^2 = \frac{8\pi G(\rho_\mathrm{m}+\rho_\mathrm{r})R^2}{3} - kc^2 + \frac{\Lambda c^2 R^2}{3}, \tag{1.7}$$

$$\frac{\mathrm{d}^2R}{\mathrm{d}t^2} = \frac{\mathrm{d}}{\mathrm{d}t}\left(\frac{\mathrm{d}R}{\mathrm{d}t}\right) = \ddot{R} = -4\pi G\left(\rho_\mathrm{m}+\rho_\mathrm{r}+\frac{3p}{c^2}\right)\frac{R}{3} + \frac{\Lambda c^2 R}{3}, \tag{1.8}$$

Proving these equations would take us a long way outside the scope of this book into what is usually graduate-level physics, but if you wish to pursue this rewarding path you might try, for example, *Relativity, Gravitation and Cosmology* by R. Lambourne for an advanced undergraduate-level introduction, or *General Relativity: An Introduction for Physicists* by M.P. Hobson, G.P. Efstathiou and A.N. Lasenby.

where ρ_m is the average matter density of the matter in the Universe, ρ_r is an equivalent matter density for radiation (derived using $E = mc^2$), G is Newton's gravitational constant, p is the pressure of the matter and radiation, and R is a function of time, $R = R(t)$, though we drop the function notation for clarity and brevity. These equations are known as the **Friedmann equations**. Both the densities and p also vary with time. Λ is known as the **cosmological constant**, and features in Einstein's field equations for general relativity. Physically, it represents an in-built tendency of space to expand (or, for $\Lambda < 0$, contract). Some special cases are fairly simple: for example, if $k = \Lambda = 0$, then $R(t) \propto t^{2/3}$ in a matter-dominated universe, or $R(t) \propto t^{1/2}$ in a radiation-dominated universe.

We can derive Equation 1.8 from Equation 1.7 by differentiation. This will give us a term involving $\mathrm{d}(\rho_\mathrm{m}+\rho_\mathrm{r})/\mathrm{d}t$, but we could treat a part of the Universe as a box of gas, and use the conservation of energy to show that the change in energy density equals the $p\,\mathrm{d}V$ work, i.e. $\mathrm{d}((\rho_\mathrm{m}+\rho_\mathrm{r})c^2R^3) = -p\,\mathrm{d}(R^3)$. Therefore $\mathrm{d}((\rho_\mathrm{m}+\rho_\mathrm{r})c^2R^3)/\mathrm{d}t = -p\,\mathrm{d}(R^3)/\mathrm{d}t$.

Exercise 1.3 Derive Equation 1.8 from Equation 1.7, using the conservation of energy. ■

(The issue of $p\,\mathrm{d}V$ work is slightly more subtle in general relativity, since it's not immediately clear what the work is done against, but the full relativistic calculation gives the same result.)

In the next few sections, we shall explore some of the surprising aspects of this expanding spacetime model, before returning to Olbers' profound paradox in the next chapter.

1.4 Redshift and time dilation

Imagine two photons being emitted at an epoch t_1 when the scale factor of the Universe was R_1. Suppose also that the photons were emitted a short time δt apart. They arrive at the Earth now at time t_0 when the scale factor is R_0. When the photons were emitted at t_1, the distance between them was $c\,\delta t$. Now, the distance between them is $(R_0/R_1)c\,\delta t$, i.e. stretched by a factor R_0/R_1 due to the

expansion of the Universe. The second photon will arrive $(R_0/R_1)\,\delta t$ later than the first. This implies that distant clocks in the Robertson–Walker universe appear time-dilated by a factor R_0/R_1, sometimes called **cosmological time dilation**. We'll find it useful to define the **dimensionless scale factor** a as

$$a = \frac{R_1}{R_0}, \tag{1.9}$$

so $a = 1$ today and $a < 1$ in the past.

A similar argument applies to the photons themselves. Treating them this time as waves, the distance between two peaks of a light wave will be expanded by the same factor R_0/R_1, i.e. the wavelength is longer, and the light is shifted to the red. We define **redshift** (symbol z) using

$$1 + z = \frac{R_0}{R_1} = \frac{1}{a} = \frac{\lambda_{\text{observed}}}{\lambda_{\text{emitted}}}, \tag{1.10}$$

where $\lambda_{\text{observed}}$ is the observed wavelength of the photon, and λ_{emitted} is the original photon wavelength when the light was emitted. Sometimes this is written as

$$z = \frac{\lambda_{\text{observed}} - \lambda_{\text{emitted}}}{\lambda_{\text{emitted}}}. \tag{1.11}$$

A high redshift means that there has been a big increase in the expansion factor since the light was emitted. Redshift is sometimes misleadingly referred to as 'recession', since a receding object would have a Doppler shift to the red. Indeed, galaxies are not stationary relative to each other, but have relative velocities up to even $1000\,\text{km}\,\text{s}^{-1}$. In astronomy these are usually known as **peculiar velocities**, and these will indeed contribute both blue and red Doppler shifts. However, cosmological redshift swamps these effects at distances beyond about $100\,\text{Mpc}$, and you should not confuse Doppler shifts with the redshift from cosmological expansion. The distance between us and a distant galaxy is getting bigger because of the expansion of the Universe, but this is a physically distinct situation to a galaxy moving away in a flat, non-expanding spacetime.

One alternative to the Robertson–Walker model is the 'tired light' universe, proposed by Fritz Zwicky in 1929. In this model, redshift is due to photons gradually losing energy during their passage through the universe, due to some interaction with intervening matter. There are many observations that are difficult to reproduce in this model, but in particular, the experimental detection of cosmological time dilation has made this interpretation untenable. Figure 1.9 shows the decay times of supernovae as a function of redshift, which show exactly the $(1 + z)$ time dilation predicted by theory.

But to measure redshifts, we need to know λ_{emitted}. This can be done using atomic or molecular transitions that occur at particular quantized energies, and so involve the emission or absorption of photons with particular quantized wavelengths. If we can identify the transition in the distant object, we know λ_{emitted}, provided that atoms behaved in the same way in the early Universe.

But did they? And if not, how could we tell? It turns out that many characteristic atomic and molecular transitions can easily be recognized at high redshifts (see, for example, Figure 1.10), so any differences must be fairly subtle. If the strength of the electromagnetic interaction were different at early cosmic epochs, this

would change the atomic fine structure constant $\alpha = e^2/(4\pi\varepsilon_0\hbar c) \simeq 1/137$. The fractional difference in wavelength ($\delta\lambda/\lambda$) between a pair of relativistic fine structure lines is proportional to α^2, so changes in α should lead to wavelength shifts between some emission lines in distant cosmological objects.

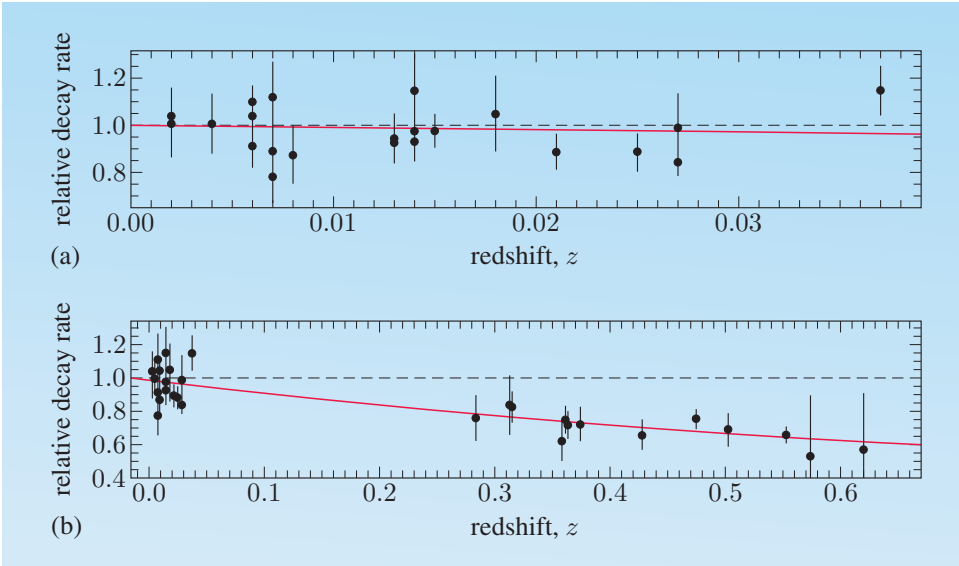

Figure 1.9 Supernova decay rates in the nearby Universe (top), and in the high-redshift Universe (bottom). The dashed line shows the tired light prediction of no time dilation, and the red line shows the $(1+z)^{-1}$ time dilation expected in the Robertson–Walker metric. The high-redshift data strongly support the expanding universe model; the measured variation is $(1+z)^{-0.97\pm0.10}$.

So far, comparisons of the atomic and molecular transitions in the early Universe with laboratory experiments have not yielded any uncontested evidence for α being any different in the early Universe; some claimed detections of changes in α have not been corroborated by other experiments, and it is clear that the experiments are both very difficult and prone to systematic errors. In terrestrial laboratories, $\dot{\alpha}/\alpha = (-2.6 \pm 3.9) \times 10^{-16}$ per year, i.e. consistent with no change. However, it remains possible that ongoing cosmological experiments will make a ground-breaking detection of a change in α. Some speculative theories allow for possible changes in α, such as supersymmetry or M-theory. However, these theories do not (or don't yet) predict the specific variations in α with redshift that some groups have claimed, in any unique and unforced way.

1.5 Cosmological parameters

How fast is the Universe expanding?

Suppose that the distance between us and a distant galaxy is $\ell = D \times R$, where R is the current scale factor of the Universe, and D is some constant. By differentiating this, we find that ℓ is increasing at a rate

$$\frac{\mathrm{d}\ell}{\mathrm{d}t} = D\,\frac{\mathrm{d}R}{\mathrm{d}t}$$

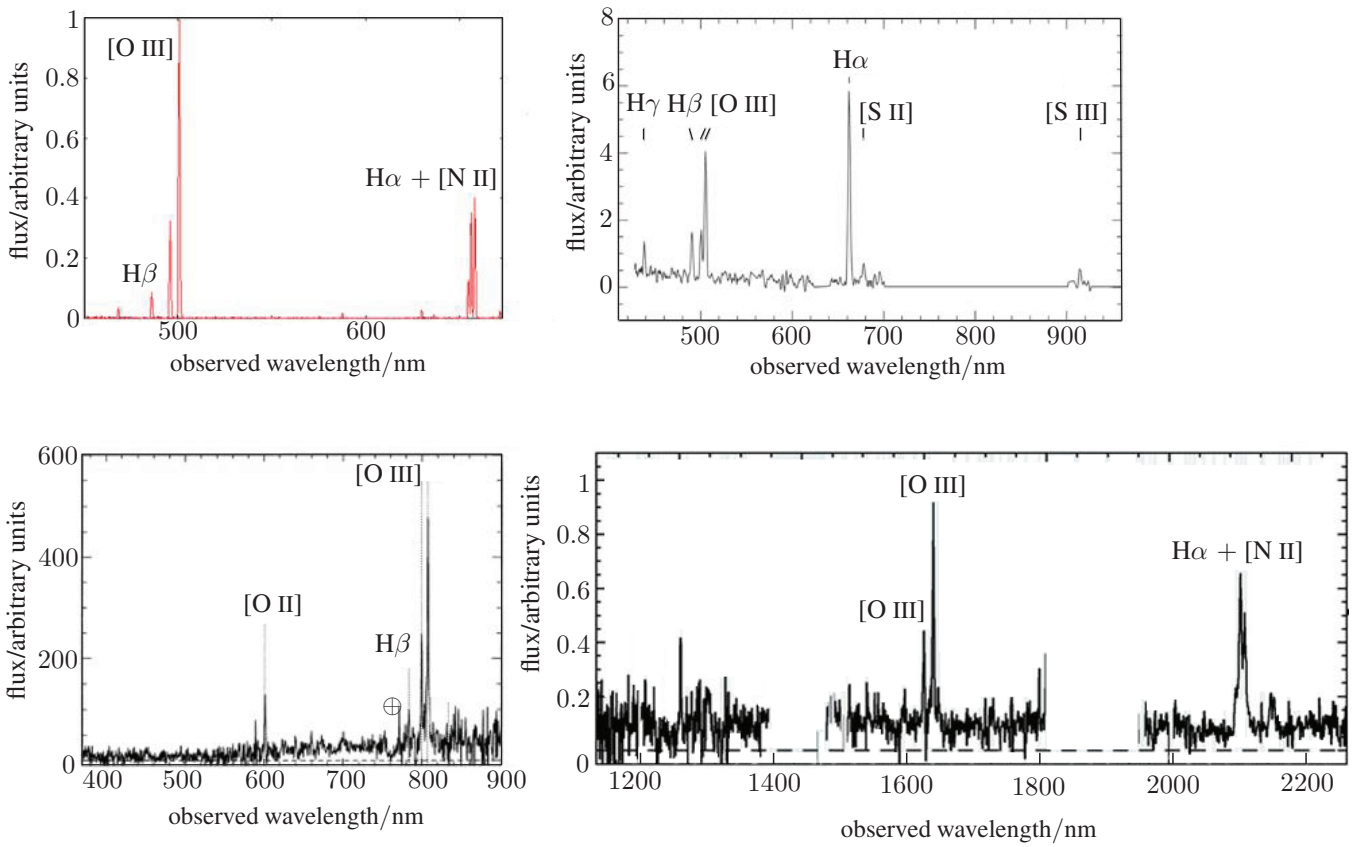

Figure 1.10 Spectra of objects in the local Universe and in the high-redshift Universe, showing many of the same characteristic spectral features. The y-axes in all the spectra are relative flux. The top left panel is a planetary nebula in our Galaxy, M57. The top right panel is an H II region in the Virgo cluster of galaxies. The bottom left panel shows the spectrum of a star-forming galaxy at a redshift of $z = 0.612$ (the $\oplus$ symbol marks absorption from the Earth's atmosphere), and the bottom right panel shows another star-forming galaxy at a redshift of $z = 2.225$. In all cases there is the characteristic [O III] emission line doublet at a rest-frame wavelength of $495.9, 500.7$ nm, as well as other emission lines such as Hα 656.3 nm, Hβ 486.1 nm, [N II] $654.8, 658.4$ nm. The bottom right panel has the emission lines redshifted into the near-infrared range, in which only certain regions of the spectrum are available, for reasons of atmospheric transparency.

because of the expansion of the Universe. But $D = \ell/R$, so

$$\frac{\mathrm{d}\ell}{\mathrm{d}t} = \frac{\ell}{R}\frac{\mathrm{d}R}{\mathrm{d}t} = \ell \times \left(\frac{1}{R}\frac{\mathrm{d}R}{\mathrm{d}t}\right) = \ell \times H,$$

where

$$H = \dot{R}/R \tag{1.12}$$

is known as the **Hubble parameter**, whose current value is known as H_0. If we regard $\mathrm{d}\ell/\mathrm{d}t$ as an *apparent* recession velocity v, then we have

$$v = \ell \times H, \tag{1.13}$$

i.e. the apparent recession velocity v is proportional to distance ℓ, but recall the warnings in Section 1.4. Sometimes this apparent flow is called the **Hubble flow**.

Beware: H is frequently (but misleadingly) known as the **Hubble constant** (Hubble constant is a fair description of H_0, however). Although it's virtually constant over our lifetimes, it certainly isn't constant over the history of the Universe. In some sense, H_0 is a measure of the current expansion rate of the Universe, and it has the value $72 \pm 3\,\mathrm{km\,s^{-1}\,Mpc^{-1}}$, or about $2 \times 10^{-18}\,\mathrm{s^{-1}}$. This is also sometimes written as $H_0 = 100h\,\mathrm{km\,s^{-1}\,Mpc^{-1}}$, with $h = 0.72 \pm 0.03$. This may seem deliberately obtuse, but the Hubble parameter is so fundamental that it affects many other cosmological measurements, so some observational cosmologists opt to quote their results in terms of h.

If we divide Equation 1.7 by R^2, we obtain

$$H^2 = \left(\frac{\dot{R}}{R}\right)^2 = \frac{8\pi G(\rho_\mathrm{m} + \rho_\mathrm{r})}{3} + \frac{\Lambda c^2}{3} - \frac{kc^2}{R^2}. \tag{1.14}$$

The terms on the right-hand side drive the expansion of the Universe. It's common in cosmology to define their fractional contributions:

$$\Omega_\mathrm{m} = \frac{8\pi G\rho_\mathrm{m}}{3H^2}, \tag{1.15}$$

$$\Omega_\mathrm{r} = \frac{8\pi G\rho_\mathrm{r}}{3H^2}, \tag{1.16}$$

$$\Omega_\Lambda = \frac{\Lambda c^2}{3H^2}, \tag{1.17}$$

$$\Omega_k = \frac{-kc^2}{R^2H^2}, \tag{1.18}$$

where the subscript 'm' stands for 'matter' and the subscript 'r' stands for 'radiation'. Equation 1.14 then implies that

$$\Omega_\mathrm{m} + \Omega_\mathrm{r} + \Omega_\Lambda + \Omega_k = 1. \tag{1.19}$$

We can also define $\Omega_\mathrm{total} = \Omega_\mathrm{m} + \Omega_\mathrm{r} + \Omega_\Lambda = 1 - \Omega_k$. All these Ω parameters, known as **density parameters**, are functions of time, except in a few special cases. Figure 1.11 shows how the density parameters varied with the scale factor of the Universe. As with the Hubble parameter, we shall use a subscript 0 for the present-day value, e.g. $\Omega_{\Lambda,0} = \Lambda c^2/(3H_0^2)$. However, be warned that many textbooks omit 0 subscripts for the present-day Ω values.

It's also useful to define a critical density ρ_crit such that

$$\Omega_\mathrm{m} = \frac{\rho_\mathrm{m}}{\rho_\mathrm{crit}}, \tag{1.20}$$

so that

$$\rho_\mathrm{crit} = \frac{3H^2}{8\pi G}, \tag{1.21}$$

(we'll explain below why this is 'critical').

Historically, another notation has been used, which is now out of favour: $q_0 = -(R\ddot{R}/\dot{R}^2)_0 = \frac{1}{2}\Omega_{\mathrm{m},0} - \Omega_{\Lambda,0}$ and $\sigma_0 = \Omega_{\mathrm{m},0}/2$. Besides mentioning them here, we won't use this notation in this book.

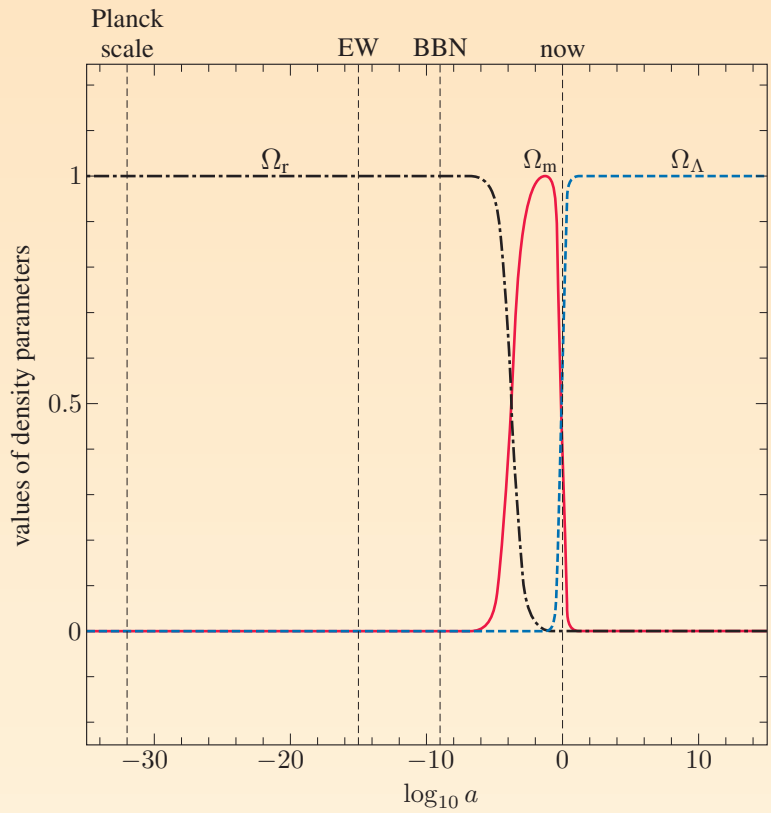

Figure 1.11 Past and future variations in the density parameters given the present-day WMAP cosmological parameters, with dimensionless scale factor $a = R/R_0$. Some key times are marked: the Planck scale, the epoch of electroweak symmetry breaking (EW), Big Bang nucleosynthesis (BBN) and the present.

Matter densities are often expressed relative to this critical density. For example, the baryon density of the Universe, ρ_b, is sometimes written as

$$\Omega_b = \frac{\rho_b}{\rho_{crit}}. \tag{1.22}$$

The matter density of the Universe can be expressed as

$$\begin{aligned}\rho_m &= \Omega_m \, \rho_{crit} = 1.8789 \times 10^{-26} \, \Omega_m h^2 \, \mathrm{kg\,m^{-3}} \\ &= 2.7752 \times 10^{11} \, \Omega_m h^2 \, \mathrm{M_\odot \, Mpc^{-3}},\end{aligned} \tag{1.23}$$

where $1\,\mathrm{M_\odot}$ is the mass of the Sun.

We shall see in later chapters that most of the matter content of the Universe is **dark matter** that neither absorbs nor emits light. Dark matter appears to interact only (or very nearly only) through gravitation, and its only observational consequences so far have been via its gravitational effects.

The current experimental values from the WMAP satellite (which we shall meet later) are

$$\Omega_{m,0} \, h^2 = 0.1326 \pm 0.0063, \tag{1.24}$$

$$\Omega_{\Lambda,0} = 0.742 \pm 0.030, \tag{1.25}$$

$$\Omega_{b,0} \, h^2 = (2.273 \pm 0.062) \times 10^{-2}. \tag{1.26}$$

We'll show in Chapter 2 that the contribution from radiation and neutrinos gives

$$\Omega_{r,0} \, h^2 \simeq 4.2 \times 10^{-5}. \tag{1.27}$$

The value of $\Omega_{\mathrm{r},0}$ is therefore negligible, and we'll usually assume that it's zero in this book. Note that WMAP doesn't constrain $\Omega_{\mathrm{m},0}$ on its own, but rather constrains the product of $\Omega_{\mathrm{m},0}$ with the Hubble parameter squared.

1.6 The age of the Universe

How old is the Universe? And how long does it take light from distant galaxies to reach us?

It is a quite astonishing feat of modern precision cosmology that we know the time since the Big Bang to better than a few per cent accuracy. To see how this is calculated, we need to relate the redshift z to the age of the Universe at that epoch, using only present-day observable quantities. The Hubble parameter H is closely related to $\mathrm{d}z/\mathrm{d}t$:

$$\begin{aligned} H = \frac{1}{R}\frac{\mathrm{d}R}{\mathrm{d}t} = \frac{R_0}{R}\frac{\mathrm{d}(R/R_0)}{\mathrm{d}t} &= (1+z)\frac{\mathrm{d}(1/(1+z))}{\mathrm{d}t} \\ &= (1+z)\frac{\mathrm{d}(1/(1+z))}{\mathrm{d}z}\frac{\mathrm{d}z}{\mathrm{d}t} \\ &= \frac{-1}{1+z}\frac{\mathrm{d}z}{\mathrm{d}t}. \end{aligned} \tag{1.28}$$

Next, we re-cast Equation 1.14 in terms of $-kc^2$ (assuming $\Omega_{\mathrm{r}} = 0$):

$$-kc^2 = H^2R^2 - \frac{8\pi G\rho_{\mathrm{m}}R^2}{3} - \frac{\Lambda c^2R^2}{3}. \tag{1.29}$$

In particular, at the present time we have

$$-kc^2 = H_0^2R_0^2 - \frac{8\pi G\rho_{\mathrm{m},0}R_0^2}{3} - \frac{\Lambda c^2R_0^2}{3}, \tag{1.30}$$

where $\rho_{\mathrm{m},0}$ is the present-day matter density. Clearly, the right-hand sides of Equations 1.29 and 1.30 must be equal. But $\rho_{\mathrm{m}} = \rho_{\mathrm{m},0} \times R_0^3/R^3$, so

$$H^2R^2 - \frac{8\pi G\rho_{\mathrm{m},0}R_0^3}{3R} - \frac{\Lambda c^2R^2}{3} = H_0^2R_0^2 - \frac{8\pi G\rho_{\mathrm{m},0}R_0^2}{3} - \frac{\Lambda c^2R_0^2}{3}.$$

We can express this in terms of the present-day density parameters $\Omega_{\mathrm{m},0}$ and $\Omega_{\Lambda,0}$ using Equations 1.15 and 1.17. After rearranging, this gives

$$\left(\frac{H}{H_0}\right)^2 = \frac{R_0^2}{R^2} + \Omega_{\mathrm{m},0}\left(\frac{R_0^3}{R^3} - \frac{R_0^2}{R^2}\right) + \Omega_{\Lambda,0}\left(1 - \frac{R_0^2}{R^2}\right). \tag{1.31}$$

We can simplify this using $1 + z = R_0/R$, which gives

$$\begin{aligned} \left(\frac{H}{H_0}\right)^2 = (1+z)^2 &+ \Omega_{\mathrm{m},0}\left\{(1+z)^3 - (1+z)^2\right\} \\ &+ \Omega_{\Lambda,0}\left\{1 - (1+z)^2\right\}, \end{aligned} \tag{1.32}$$

which can be rearranged to give

$$\left(\frac{H}{H_0}\right)^2 = (1+z)^2(1+z\,\Omega_{\mathrm{m},0}) - z(2+z)\,\Omega_{\Lambda,0}. \tag{1.33}$$

Finally, using Equation 1.28, we reach

$$\left(\frac{\mathrm{d}z}{\mathrm{d}t}\right)^2 = H_0^2(1+z)^2\left\{(1+z)^2(1+z\,\Omega_{\mathrm{m},0}) - z(2+z)\,\Omega_{\Lambda,0}\right\}, \quad (1.34)$$

from which we can easily find $\mathrm{d}t/\mathrm{d}z$. Although admittedly pretty ghastly, this equation does have the advantage of using only present-day observable quantities, and we'll be referring to it several times in this book.

In general, $\mathrm{d}t/\mathrm{d}z$ can't be integrated analytically, so $t(z)$ can be calculated only by numerically integrating $\mathrm{d}t/\mathrm{d}z$. The time to $z = \infty$ is the age of the Universe, and this is shown in Figure 1.12. Equation 1.34 can also be integrated to give the time taken for light to reach us from redshift z. This is known as the **lookback time**.

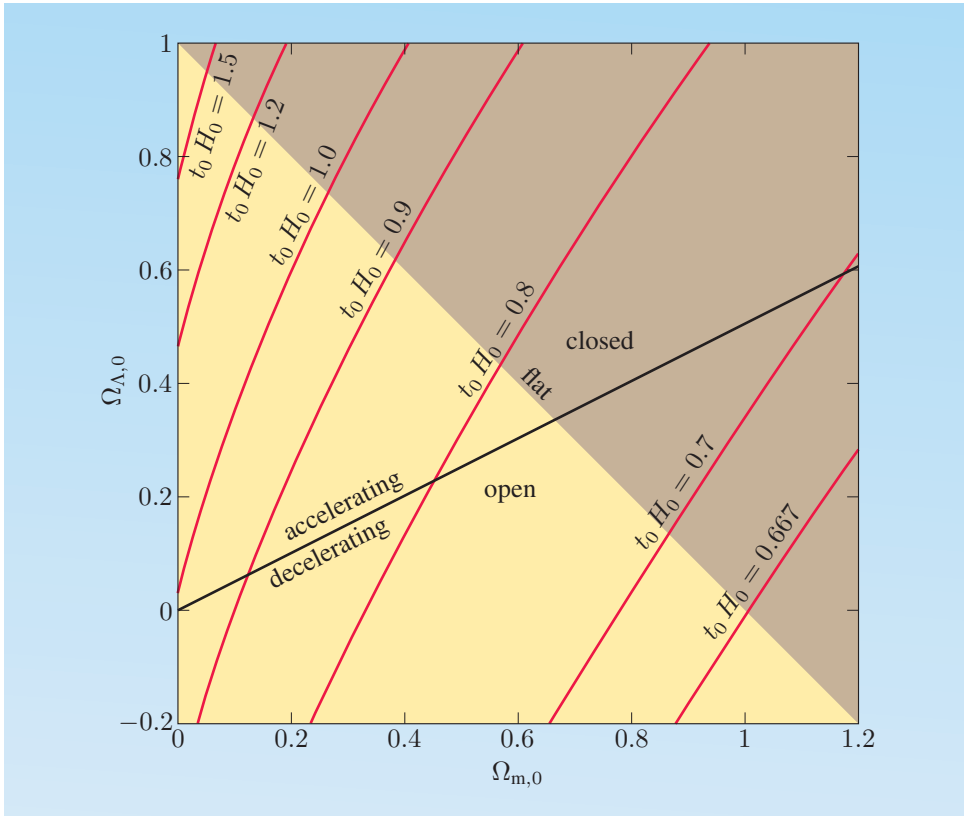

Figure 1.12 The age of the Universe times the Hubble parameter, for several cosmological models. Also shown is the spatial geometry (open, flat and closed) and whether the present-day expansion of the Universe would be accelerating or decelerating.

How does this estimate of the age of the Universe compare to the ages of the oldest objects in the Universe? There is now a well-developed theory for main sequence stellar evolution that can be used to find the ages of stars. Particularly useful are globular clusters (e.g. Figure 1.13), which are some of the oldest gravitationally-bound objects in the Universe. The stars that comprise any given globular cluster are believed to have formed at about the same time (though the ages of globular clusters vary). More luminous stars spend less time on the main sequence in the colour–magnitude diagram, so if one can find the luminosity of

the stars in a globular cluster that are just leaving the main sequence, one can infer an age for the globular cluster.

The oldest known globular cluster appears to be 12.7 ± 0.7 Gyr old. In the 1990s it was recognized that globular cluster ages are an important constraint on the age of the Universe, and therefore on the cosmological parameters that control the geometry and fate of the Universe (Figure 1.12). But as we shall see in the next section, there seemed to be very good reasons to expect that we live in a Universe with $\Omega_{\mathrm{m},0} = 1$ and $\Lambda = 0$, which as you will see turns out to be significantly younger, so these stars appeared to be older than the Universe.

Figure 1.13 The globular star cluster M80. Most of its stars are older and redder than our Sun.

Exercise 1.4 Starting from Equation 1.33, or otherwise, show that in an $\Omega_{\mathrm{m}} = 1$, $\Lambda = 0$ universe,

$$\frac{R}{R_0} = \left(\frac{t}{t_0}\right)^{2/3}. \tag{1.35}$$

Exercise 1.5 Using Equation 1.35, show that the age of the Universe in an $\Omega_{\mathrm{m}} = 1$, $\Lambda = 0$ model is $t_0 = 2/(3H_0)$, and evaluate the age in Gyr for the value of H_0 in Section 1.5. A spacetime that expands in this way is sometimes called the **Einstein–de Sitter model**. ■

1.7 The flatness problem

In this section we shall introduce you to a profound, and as yet unsolved, problem in cosmology. We have already noted that the density parameters in general depend on time. For example, what was Ω_{m} at a redshift of $z = 1000$ (about the redshift of the cosmic microwave background)? Let's assume for now that $\Lambda = 0$, so Ω_Λ is always zero, and $\Omega_{\mathrm{m}} = 1 - \Omega_k$. Equation 1.18 can be modified to give the current value of Ω_k,

$$\Omega_{k,0} = \frac{-kc^2}{R_0^2 H_0^2},$$

and dividing this into Equation 1.18 gives

$$\frac{\Omega_k(z)}{\Omega_{k,0}} = \frac{R_0^2 H_0^2}{R^2 H^2} = (1+z)^2 \left(\frac{H_0}{H}\right)^2.$$

Now we know how to relate H to z (Equation 1.33), so we can find how Ω_k and Ω_{m} evolve.

First, if $\Lambda = 0$ and $\Omega_{\mathrm{m},0} = 1$, then $\Omega_{k,0} = 0$. But this can happen only if $k = 0$, so Ω_k must always be zero, and $\Omega_{\mathrm{m}} = 1$ at all times.

But if $\Lambda = 0$ and $\Omega_{\mathrm{m},0} = 0.7$, then at $z = 1000$, $\Omega_{\mathrm{m}} = 0.9996$. As redshift increases, Ω_k tends to zero and Ω_{m} tends to 1. About one second after the Big Bang, $\Omega_{\mathrm{m}} = 1 - 10^{-15}$. So if the present-day value of Ω_{m} is not 1, it must have had only a very tiny offset from 1 in the early Universe. What could cause it to be so close to 1, but not quite equal to 1?

This fine-tuning problem is worse if we include a non-zero Λ. If $\Omega_{\Lambda,0} = 0.7$ and $\Omega_{\mathrm{m},0} = 0.3$, then at $z = 1000$ their values were $\Omega_\Lambda = 3.3 \times 10^{-9}$ and $\Omega_{\mathrm{m}} = 0.999\,999\,996$.

Figure 1.14 shows how the Ω parameters depend on redshift, for various cosmological models. If $\Omega_{\rm m} = 1$ and $\Omega_\Lambda = 0$, then they keep these values throughout the history of the Universe. This would remove the need to explain the cosmological fine-tuning in the Ω parameters, and led to the expectation among at least some astronomers that the likely values are $\Omega_{\rm m,0} = 1$ and $\Omega_{\Lambda,0} = 0$. However, there is now good experimental evidence to reject this particular cosmological model, so we are left with the problem: what caused the fine-tuning in the early Universe?

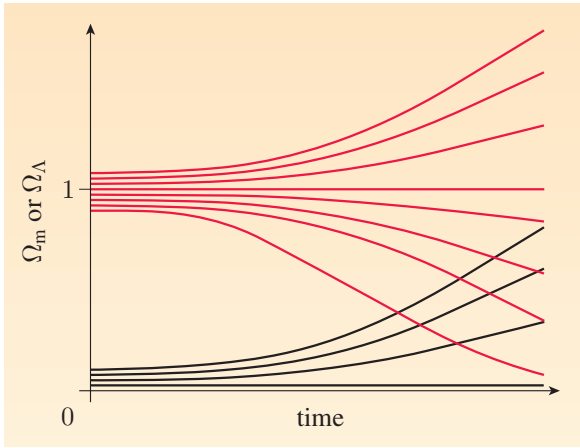

Figure 1.14 Schematic illustration of the variation of the density parameters $\Omega_{\rm m}$ (upper, red lines) and Ω_Λ (lower, black lines) with time, for various cosmological models. Note that the time-dependence of a density parameter for any given starting point also depends on the starting values of the other density parameters.

One possible solution for the smallness of Ω_k, or rather a class of possible solutions, is inflation, which we shall meet in later chapters. But it is by no means certain that this is the correct solution. Inflation also does not offer any clear explanation for the fine-tuning of Ω_Λ. There may be Nobel prizes to be had for successful insights into the origin of Ω_Λ.

1.8 Distance in a warped spacetime

In 1963, Maarten Schmidt and Bev Oke made an astonishing discovery: the extraterrestrial radio source 3C273 is at what was then an unprecedentedly vast distance, a redshift of $z = 0.158$. Suddenly astronomers realized that telescopes could explore a much bigger volume of the Universe than had been supposed, and see objects as they were much earlier in the history of the Universe. This produced great excitement and optimism in cosmology. This also meant that 3C273 must be extremely luminous. We shall explore the causes of this prodigious luminosity in later chapters.

Using $\mathrm{d}z/\mathrm{d}t$ from Section 1.6, then integrating numerically with the cosmological parameters from Section 1.5, it turns out that the light from 3C273 has taken 1.9 billion years to reach us, which is about 14% of the age of the Universe. Does this mean that 3C273 is 1.9 billion light-years away?

It turns out that 'distance' is a surprisingly tricky concept to define in an expanding spacetime. Figure 1.15 shows some of the problems. Do we mean the distance that the light has travelled (B to C)? Or do we mean the distance that 3C273 was at when the light was emitted (B to A)? Or do we mean the distance that 3C273 is at now (D to C)?

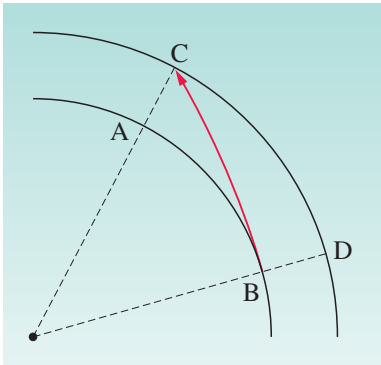

Figure 1.15 Different options for measuring cosmological distances in an expanding universe.

Cosmologists have settled on a convention to use D to C (neglecting any peculiar velocities), in the preferred reference frame of the Robertson–Walker metric. This distance is known as the **comoving distance**. The comoving distance to 3C273 is about 637 Mpc, or about 2.1 billion light-years. This is longer than the light-travel distance, because the space has been expanding since the light was emitted, and 3C273 is now further away than when it emitted the light. Figure 1.16 illustrates how the Universe looks in **proper coordinates** (proper distances are those that would be measured by a tape measure at a fixed time in the cosmic rest frame), and in comoving coordinates.

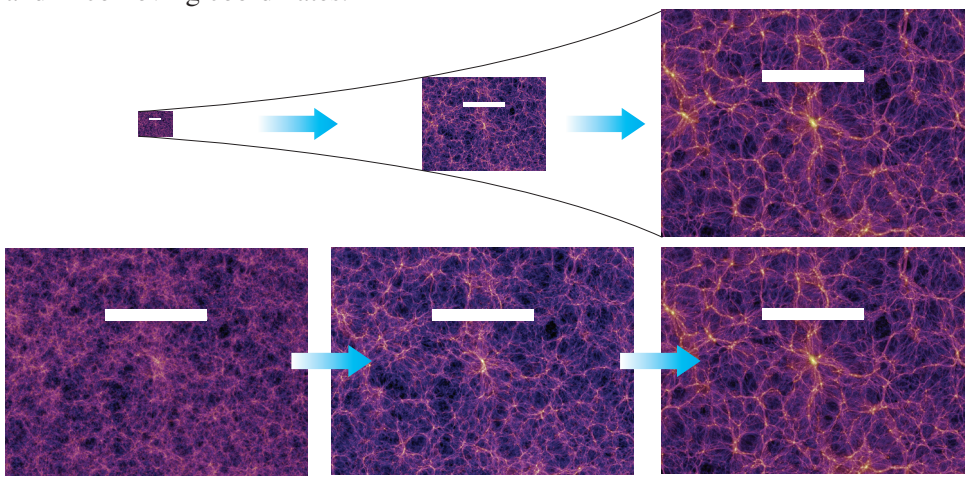

Figure 1.16 A simulation of the expanding Universe as seen in proper coordinates and in comoving coordinates. The panels show a simulation of a segment of the Universe at redshifts of $z = 5.7$ (left), $z = 1.4$ (centre) and $z = 0$ (right). The upper panels are shown in proper coordinates, while the lower panels are shown in comoving coordinates. A white bar shows a comoving length of $125/h$ Mpc. Note also the gradual increase in large-scale structure in this simulation with time, which we shall return to in later chapters.

To calculate the comoving distance to a cosmological object, we can use the Robertson–Walker metric, Equation 1.6. We want to know the radial distance between us and a distant object, at a fixed coordinate time $t = t_0$ (i.e. the present), perhaps imagining a tape measure stretched between us and it, which we read at the time $t = t_0$. Therefore $\mathrm{d}t = 0$ and $\mathrm{d}\theta = \mathrm{d}\phi = 0$. The remaining non-zero terms of Equation 1.6 are

$$\mathrm{d}s^2 = \frac{-R^2(t_0)\,\mathrm{d}r^2}{1 - kr^2}.$$

This is -1 times the square of a spatial separation. We define the comoving distance d_{comoving} via

$$\mathrm{d}d_{\mathrm{comoving}} = \frac{R(t_0)\,\mathrm{d}r}{\sqrt{1 - kr^2}} = \frac{R_0\,\mathrm{d}r}{\sqrt{1 - kr^2}} \tag{1.36}$$

(with apologies for the profusion of the letter d) so that

$$d_{\mathrm{comoving}} = R_0 \int_0^r \frac{\mathrm{d}r'}{\sqrt{1 - kr'^2}}. \tag{1.37}$$

This integral has a standard solution, depending on the value of k:

$$d_{\text{comoving}} = \begin{cases} R_0 \sin^{-1} r & \text{if } k = +1, \\ R_0 r & \text{if } k = 0, \\ R_0 \sinh^{-1} r & \text{if } k = -1. \end{cases} \tag{1.38}$$

Now, it's all very well imagining imaginary tape measures, but how can we relate this to real observable quantities? To find out, consider the light ray arriving at the Earth from the distant object. Light rays have $\mathrm{d}s = 0$, and the motion of this light ray is purely radial, so $\mathrm{d}\theta = \mathrm{d}\phi = 0$. The motion of the light ray is therefore just

$$\frac{R(t)\,\mathrm{d}r}{\sqrt{1-kr^2}} = c\,\mathrm{d}t. \tag{1.39}$$

Our aim is to calculate d_{comoving} following Equation 1.38.

In general, $R(t)$ can't be expressed analytically, though there are a few analytic special cases (e.g. $R(t) \propto t^{2/3}$ for a matter-dominated universe with $\Omega_{\text{m}} = 1$ and $\Lambda = 0$). But it's more helpful to express the right-hand side of Equation 1.39 in terms of redshift, which (unlike lookback time) is directly observable. To do this, we start with the chain rule for differentiation:

$$c\,\mathrm{d}t = c\,\mathrm{d}R\,\frac{\mathrm{d}t}{\mathrm{d}R} = \frac{c\,\mathrm{d}R}{\mathrm{d}R/\mathrm{d}t} = \frac{c\,\mathrm{d}R}{RH}, \tag{1.40}$$

where we have used $H = \dot{R}/R$. Next, $R = R_0/(1+z)$, which we can differentiate to find

$$\mathrm{d}R = \frac{-R_0}{(1+z)^2}\,\mathrm{d}z.$$

Putting this into Equation 1.40 gives

$$c\,\mathrm{d}t = \frac{-c}{HR}\,\frac{R_0}{(1+z)^2}\,\mathrm{d}z = \frac{-c}{(1+z)H}\,\mathrm{d}z$$

and therefore

$$\frac{R\,\mathrm{d}r}{\sqrt{1-kr^2}} = \frac{-c\,\mathrm{d}z}{(1+z)H}. \tag{1.41}$$

The comoving distance is $\int_0^r R_0\,(1-kr'^2)^{-1/2}\,\mathrm{d}r'$ (Equation 1.37), and this is almost in the right form. $R_0 = (1+z)R$, so $R_0\,\mathrm{d}r = (1+z)R\,\mathrm{d}r$, and therefore

$$\frac{R_0\,\mathrm{d}r}{\sqrt{1-kr^2}} = \mathrm{d}d_{\text{comoving}} = \frac{-c\,\mathrm{d}z}{H}, \tag{1.42}$$

where H is a function of redshift. Therefore the comoving distance is just

$$d_{\text{comoving}} = c\int_0^z \frac{\mathrm{d}z'}{H(z')}. \tag{1.43}$$

But we know H in terms of z and the observed cosmological parameters — we found this back in Equation 1.33. Putting this in here, and using $R_0/R = 1+z$, we get

$$\mathrm{d}d_{\text{comoving}} = \frac{-c}{H_0}\,\frac{\mathrm{d}z}{\sqrt{(1+z)^2(1+z\,\Omega_{\text{m},0}) - z(2+z)\,\Omega_{\Lambda,0}}},$$

thus

$$d_{\text{comoving}} = \frac{c}{H_0}\int_0^z \frac{\mathrm{d}z'}{\sqrt{(1+z')^2(1+z'\,\Omega_{\text{m},0}) - z'(2+z')\,\Omega_{\Lambda,0}}}. \qquad (1.44)$$

(We have integrated the previous differential from z to 0, but used its minus sign to swap the limits and obtain a positive integral.) There are a few special cases where this integral comes out as a relatively simple expression, such as when $\Lambda = 0$ and $\Omega_{\text{m}} = 1$:

$$d_{\text{comoving}} = \frac{2c}{H_0}\left(1 - (1+z)^{-1/2}\right) \textit{ only for } \Omega_{\text{m}} = 1,\ \Lambda = 0. \qquad (1.45)$$

1.9 The edge of the observable Universe

How big is the observable Universe today? If we lived in a flat, unexpanding space, the observable Universe would be the region of the Universe that could have sent us a light signal. The radius would be ct_0, where t_0 is the age of the Universe. This radius would be increasing at a speed c.

In the Robertson–Walker expanding universe, this is different in a rather astonishing way. First, we'll calculate the size of the observable Universe. This size is the same in comoving coordinates and in proper coordinates, provided that we're referring to the size at time $t = t_0$ (i.e. now) when the scale factor is $R = R_0$.

The size of the observable Universe is therefore the comoving radius in Equation 1.44 as redshift z tends to infinity. In general, this comes out as a number times c/H_0. For an $\Omega_{\text{m}} = 1$ and $\Lambda = 0$ universe, you can see from Equation 1.45 that the radius of the observable Universe is $2c/H_0$, or about 8300 Mpc for the currently-accepted value of H_0 in Section 1.5. For the currently-accepted values of the density parameters in Section 1.5, the radius of the observable Universe comes out at about $3.53c/H_0$. The volume enclosed is sometimes referred to as the **Hubble volume**.

Next, we'll calculate how fast this observable Universe is growing, in proper distances rather than comoving distances. Again, we take the time now to be t_0 and the current scale factor to be R_0. Suppose that we see a distant object at a redshift z and a proper distance $R_0 r$. After a time δt, the time will be $t_1 = t_0 + \delta t$, and the new scale factor of the Universe will be R_1. Therefore the new proper distance to this distant object will be

$$R_1 r = R_0 r + \left(\frac{\mathrm{d}R}{\mathrm{d}t}\,\delta t\right) r \simeq R_0 r + (R_0 H_0\,\delta t) r.$$

Therefore the rate of change of proper distance is

$$\frac{\mathrm{d}(Rr)}{\mathrm{d}t} \simeq \frac{R_1 r - R_0 r}{\delta t} = R_0 H_0 r, \qquad (1.46)$$

i.e. just H_0 times the current proper distance. This is one sense in which the Hubble parameter is measuring the rate of the expansion of the Universe.

So, for the currently-accepted values of the density parameters in Section 1.5, the observable Universe is getting bigger at an astonishing rate of $(3.53c/H_0) \times H_0 = 3.53c$. In Section 1.5 we met Equation 1.46 in a different

guise (Equation 1.13), but warned that the left-hand side is not a *recession* velocity, but rather an *apparent* recession. Here, you see our reason for this warning! An object moving through a flat, unexpanding space has a maximum speed of c, but an expanding spacetime is a very different physical situation, and the maximum cosmological apparent 'recession' speed in our Universe is currently about $3.53c$.

1.10 Measuring distances and volumes

Redshift is one way of measuring distances, but to convert redshift into a distance, we need to know the cosmological parameters, especially H_0. If we want to measure these fundamental cosmological parameters, we need independent ways of measuring distances.

One useful distance measure is the **angular diameter distance**. If an object has a known size D, and subtends an angle θ in radians, then the angular diameter distance is

$$d_{\mathrm{A}} = \frac{D}{\theta}. \tag{1.47}$$

(Compare Figure 1.2, in which r takes the place of d_{A}.)

Another useful measure is the **proper motion distance**. If an object has a known transverse velocity u (i.e. motion in the plane of the sky), and has an observed angular motion of $\mathrm{d}\theta/\mathrm{d}t$, then the proper motion distance is defined as

$$d_{\mathrm{M}} = \frac{u}{\mathrm{d}\theta/\mathrm{d}t}. \tag{1.48}$$

Finally, we can also define the **luminosity distance**. If an object has a known luminosity L, and the observed flux is S, then the luminosity distance is

$$d_{\mathrm{L}} = \left(\frac{L}{4\pi S}\right)^{1/2}. \tag{1.49}$$

These three approaches to measuring distance give the same answer in a flat, unexpanding space, but they are surprisingly different in the Robertson–Walker metric. Figure 1.17 illustrates how these distances are constructed in Robertson–Walker universes. As usual, we use t_0 and R_0 for the current time and current scale factor, respectively. Suppose that photons are emitted from a distant object of size D at a time t_1, when the scale factor was R_1. From the figure, we see that $D = R_1 r\theta$, so $d_{\mathrm{A}} = R_1 r$.

Next, suppose that another object at the same redshift is moving with a proper transverse velocity u, and is seen to move at an angular speed $\mathrm{d}\theta/\mathrm{d}t$, as in Equation 1.48. Here, the cosmological time dilation first noted in Section 1.4 comes into play. If t' is the time measured when the photons are emitted, then $\mathrm{d}t'/\mathrm{d}t = R_1/R_0$. The proper velocity is

$$u = \frac{\mathrm{d}D}{\mathrm{d}t'} = \frac{\mathrm{d}(R_1 r\theta)}{\mathrm{d}t'},$$

and substituting this into Equation 1.48, we find $d_{\mathrm{M}} = R_0 r$. Note that when $k = 0$, this equals the comoving distance (compare Equation 1.38).

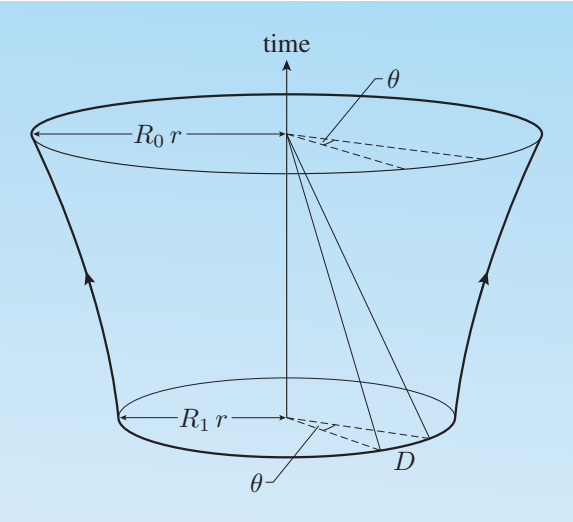

Figure 1.17 Light rays in the Robertson–Walker metric, for illustrating distance measures.

Finally, suppose that an object at this redshift has a bolometric luminosity L (where 'bolometric' means the total over all wavelengths). The photons are distributed over a sphere with a proper area of $4\pi(R_0 r)^2$ (see Figure 1.17). The energy emitted in a time $\mathrm{d}t'$ will be $L\,\mathrm{d}t'$, but the redshifting will reduce the energy received by a factor of R_1/R_0. Therefore the flux received will be

$$S = \frac{L\,\mathrm{d}t'\,R_1/R_0}{\mathrm{d}t} \times \frac{1}{4\pi(R_0 r)^2} = L\,\frac{\mathrm{d}t'}{\mathrm{d}t}\,\frac{R_1}{R_0}\,\frac{1}{4\pi}\,\frac{1}{R_0^2\,r^2}.$$

But because of cosmological time dilation, $\mathrm{d}t'/\mathrm{d}t = R_1/R_0$, so

$$S = L\,\frac{R_1}{R_0}\,\frac{R_1}{R_0}\,\frac{1}{4\pi}\,\frac{1}{R_0^2\,r^2} = \frac{LR_1^2}{4\pi r^2 R_0^4} = \frac{L}{4\pi(R_0^2 r/R_1)^2}.$$

Comparing this to Equation 1.49, we see that $d_\mathrm{L} = R_0^2 r/R_1$. It would be wonderful if comparing these three distance measures for a single object gave us constraints on the cosmological parameters. It's perhaps a little disappointing, then, that they are all closely related. Using $1 + z = R_0/R_1$, we find that

$$d_\mathrm{L} = (1+z)d_\mathrm{M} = (1+z)^2 d_\mathrm{A}, \tag{1.50}$$

independent of the cosmological parameters. The constraints on the cosmological parameters can instead be gleaned from how these distance measures vary with redshift. Figure 1.18 shows how the angular diameter distance varies with redshift, for various cosmological models.

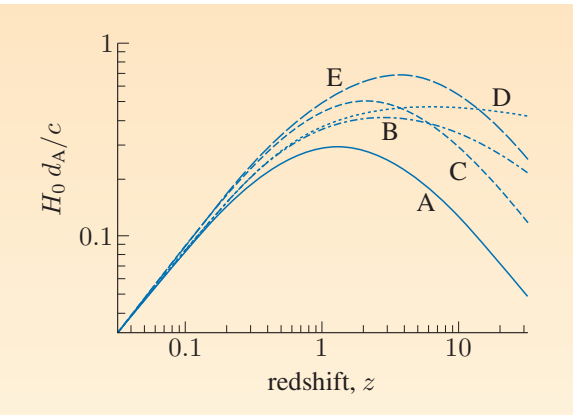

Figure 1.18 The variation of angular diameter distance with redshift, for the following cosmological models. A: $\Omega_\mathrm{m} = 1$, $\Lambda = 0$. B: $\Omega_{\mathrm{m},0} = 0.1$, $\Lambda = 0$. C: $\Omega_{\mathrm{m},0} = 0.1$, $\Omega_{\Lambda,0} = 0.9$. D: $\Omega_{\mathrm{m},0} = 0.01$, $\Lambda = 0$. E: $\Omega_{\mathrm{m},0} = 0.01$, $\Omega_{\Lambda,0} = 0.99$.

Again, the Robertson–Walker metric holds another surprise: the angular diameter distance d_A has a maximum value, as you can see in Figure 1.18. What does this mean? In flat unexpanding space, objects always appear smaller when they are placed further away, but in the Robertson–Walker spacetime, an object that is placed further away can appear *larger*. This is partly because the Universe was smaller when the light was emitted, so the object was then nearer to us. It's partly also to do with the geometry of the space. For example, light rays emitted on a two-dimensional spherical surface at the South pole will initially diverge, but will eventually converge again as they approach the North pole. A spherical unexpanding space would therefore still have a maximum angular diameter distance.

We shall see how these distances affect Olbers' paradox later in this book. In the meantime, the following exercise will give you a clue to how Olbers' paradox is resolved in a Robertson–Walker universe.

Exercise 1.6 How does surface brightness (flux per square degree) vary with redshift? ■

In observational astronomy we rarely measure the total luminosities of distant objects; instead, we tend to measure the redshift and the flux in a particular wavelength interval $\Delta\lambda_{\rm obs}$. Two effects change the observed flux: first, the observed wavelength interval $\Delta\lambda_{\rm obs}$ corresponds to a smaller wavelength interval in the emitted frame, because $\Delta\lambda_{\rm obs} = (1+z)\Delta\lambda_{\rm em}$; second, the distant object may emit different amounts of light at *rest* wavelengths of $\lambda_{\rm em}$ and $\lambda_{\rm obs}$. This latter effect is known as the **K-correction** for historical reasons, and we shall meet it later in this book. If the underlying spectrum is a 'power law', i.e. if the flux per unit frequency is $S_\nu \propto \nu^{-\alpha}$, then a useful expression for the luminosity is

$$\frac{L_\nu}{10^{26}\,\mathrm{W\,Hz^{-1}\,sr^{-1}}} = \frac{S_\nu}{10^{-26}\,\mathrm{W\,Hz^{-1}\,m^{-2}}}\left(\frac{d_{\rm M}}{3241\,\mathrm{Mpc}}\right)^2 (1+z)^{1+\alpha}. \quad (1.51)$$

Finally, cosmologists often use the term **comoving volume** to describe volumes with the expansion factor divided out (Figure 1.16). We shall use this many times throughout this book. Imagine a patch of sky with an angular area $\delta\Omega$ (in units, for example, of square degrees). We can convert this to a proper area at any redshift using the angular diameter distance: $\delta A = d_{\rm A}^2\,\delta\Omega$. Now imagine that we are observing a slab at redshift z with a proper area δA and proper thickness $R(1-kr^2)^{-1/2}\,\mathrm{d}r$. The proper volume will therefore be $\mathrm{d}V_{\rm proper} = \delta A \times (1-kr^2)^{-1/2} R\,\mathrm{d}r$, or

$$\mathrm{d}V_{\rm proper} = d_{\rm A}^2(z)\,\delta\Omega \times \frac{R\,\mathrm{d}r}{\sqrt{1-kr^2}}. \quad (1.52)$$

Now the comoving volume is just $\mathrm{d}V_{\rm comoving} = (1+z)^3 \times \mathrm{d}V_{\rm proper}$, so

$$\mathrm{d}V_{\rm comoving} = d_{\rm A}^2(z)\,\delta\Omega\,\frac{R\,\mathrm{d}r}{\sqrt{1-kr^2}} \times (1+z)^3. \quad (1.53)$$

There are many ways of integrating this, but one approach is to express it in terms of the proper motion distance $d_{\rm M} = R_0 r$. (Recall that in a flat universe this is equivalent to the comoving distance.) Then

$$\mathrm{d}V_{\rm comoving} = \frac{d_{\rm M}^2(z)}{\sqrt{1+\Omega_{k,0}H_0^2 d_{\rm M}^2/c^2}}\,\mathrm{d}(d_{\rm M})\,\delta\Omega. \quad (1.54)$$

We'll express this in another useful way in Chapter 6, Equation 6.26.

The function $\mathrm{d}V_{\text{comoving}}/\mathrm{d}z$ is plotted in Figure 1.19. This can be integrated to give $V_{\text{comoving}}(z)$, the total volume enclosed by a sphere with radius z centred on us. The form of the comoving volume equation depends on whether $k = 0$, $k = 1$ or $k = -1$. For reference, there are analytic solutions for the comoving volume over the whole sky, in terms of the proper motion distance d_{M}:

$$V(d_{\text{M}}) = \begin{cases} 4\pi D_{\text{H}}^3 (2\Omega_{k,0})^{-1} [(d_{\text{M}}/D_{\text{H}}) \sqrt{1 + \Omega_{k,0} d_{\text{M}}^2 / D_{\text{H}}^2} - |\Omega_{k,0}|^{-1/2} \sin^{-1}((d_{\text{M}}/D_{\text{H}}) |\Omega_{k,0}|^{1/2})] & \text{if } k = +1, \\ \frac{4}{3}\pi d_{\text{M}}^3 & \text{if } k = 0, \\ 4\pi D_{\text{H}}^3 (2\Omega_{k,0})^{-1} [(d_{\text{M}}/D_{\text{H}}) \sqrt{1 + \Omega_{k,0} d_{\text{M}}^2 / D_{\text{H}}^2} - |\Omega_{k,0}|^{-1/2} \sinh^{-1}((d_{\text{M}}/D_{\text{H}}) |\Omega_{k,0}|^{1/2})] & \text{if } k = -1, \end{cases} \tag{1.55}$$

where $D_{\text{H}} = c/H_0$ is sometimes known as the **Hubble distance**. Also, for reference, the proper motion distance can be expressed as

$$d_{\text{M}} = \begin{cases} D_{\text{H}} \dfrac{1}{|\Omega_{k,0}|^{1/2}} \sin \left[|\Omega_{k,0}|^{1/2} \displaystyle\int_0^z \left\{ (1+z)^2 (1 + \Omega_{\text{m},0} z) - z(2+z)\Omega_{\Lambda,0} \right\}^{-1/2} \mathrm{d}z \right] & \text{if } k = +1, \\ d_{\text{comoving}} & \text{if } k = 0, \\ D_{\text{H}} \dfrac{1}{|\Omega_{k,0}|^{1/2}} \sinh \left[|\Omega_{k,0}|^{1/2} \displaystyle\int_0^z \left\{ (1+z)^2 (1 + \Omega_{\text{m},0} z) - z(2+z)\Omega_{\Lambda,0} \right\}^{-1/2} \mathrm{d}z \right] & \text{if } k = -1. \end{cases} \tag{1.56}$$

Equation 1.44 gives the expression for d_{comoving}. Remember that proper motion distance d_{M} is equal to comoving distance d_{comoving} *only when* $k = 0$.

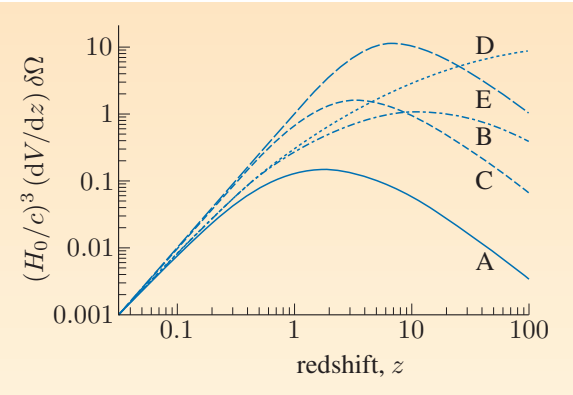

Figure 1.19 The variation of the comoving volume derivative $\mathrm{d}V/\mathrm{d}z$ with redshift, for the various cosmological models in Figure 1.18, and for an angular area on the sky of $\delta\Omega$.

1.11 The fate of the Universe

The cosmological parameters in Section 1.5 can also tell us the fate of the Universe. An extraordinary consequence of the success of the Robertson–Walker model is that we know the ultimate fate of the atoms in our bodies, at least up to about the year AD 10^{35}.

We can again re-cast Equation 1.14, this time by changing the variables to $a = 1/(1+z) = R/R_0$ and $\tau = H_0 t$. This comes out as

$$\left(\frac{\mathrm{d}a}{\mathrm{d}\tau}\right)^2 = 1 + \Omega_{\text{m},0} \left(\frac{1}{a} - 1\right) + \Omega_{\Lambda,0}(a^2 - 1).$$

This differential equation can be solved numerically, and the predicted fate of the Universe is shown in Figure 1.20 as a function of $\Omega_{m,0}$ and $\Omega_{\Lambda,0}$. The cosmological parameters in Section 1.5 are very clearly in the regime of expanding forever.

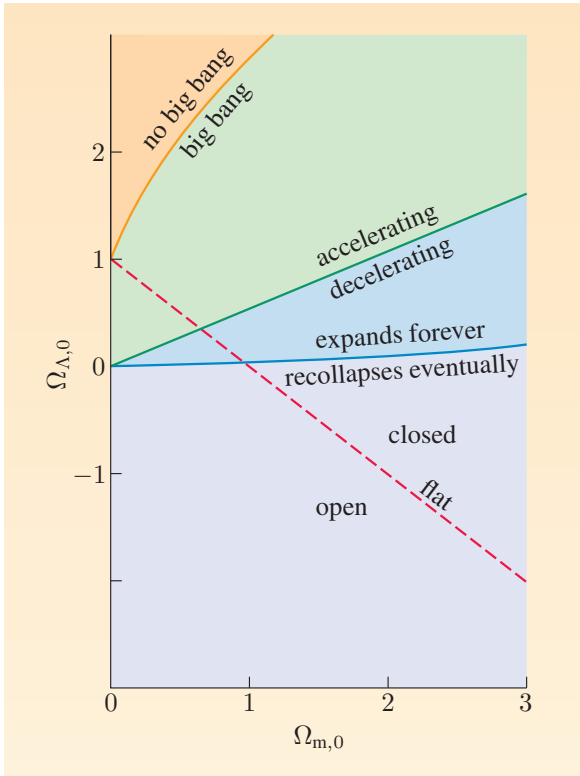

Figure 1.20 The predicted fate of the Universe as a function of the present-day cosmological density parameters.

What will this be like? The Universe will become increasingly sparse, as the matter density decreases and Ω_m tends to zero. The cosmological constant will then dominate, and the Universe will tend to the $\Omega_\Lambda = 1$ model. Equation 1.14 will reduce to

$$H^2 = \frac{\Lambda c^2}{3}$$

so the Hubble constant will, finally, be truly a constant. The expansion will be exponential, as you can see from substituting $H = \dot{R}/R$ into the equation above:

$$\frac{1}{R}\frac{\mathrm{d}R}{\mathrm{d}t} = \sqrt{\frac{\Lambda c^2}{3}},$$

which has the solution $R \propto \mathrm{e}^{ct\sqrt{\Lambda/3}}$. This is sometimes known as **de Sitter spacetime**.

This exponential expansion has a curious consequence. Regions of the Universe that were once in causal contact eventually lose contact with each other, as the rapidly expanding space makes it impossible for even light signals to pass between them. To show this, imagine a light signal being sent out in this universe. How far can it get? The light signal will be in an exponentially expanding universe, so in a sense it will go infinitely far, but if we normalize our distances by the scale factor, then we'll see that the light signal reaches only a finite *comoving* region.

Light signals still satisfy Equation 1.39, i.e. $R(t)\,\mathrm{d}r = c\,\mathrm{d}t$ (note that $k = 0$ because $\Omega_k = 1 - \Omega_\mathrm{m} - \Omega_\Lambda = 1 - 0 - 1 = 0$), but this time $R(t)$ is very different. If we set $R(t) = R_1$ at a time $t = t_1$, then

$$\frac{R(t)}{R(t_1)} = \frac{R(t)}{R_1} = \frac{\mathrm{e}^{ct\sqrt{\Lambda/3}}}{\mathrm{e}^{ct_1\sqrt{\Lambda/3}}} = \mathrm{e}^{c(t-t_1)\sqrt{\Lambda/3}}.$$

If we treat $R_1 r$ as our choice of comoving distance, then we have

$$R_1\,\mathrm{d}r = c\,\mathrm{e}^{-c(t-t_1)\sqrt{\Lambda/3}}\,\mathrm{d}t$$

so

$$R_1 r = \int_{t=t_1}^{\infty} c\,\mathrm{e}^{-c(t-t_1)\sqrt{\Lambda/3}}\,\mathrm{d}t = \frac{c}{c\sqrt{\Lambda/3}} = \sqrt{\frac{3}{\Lambda}} = \frac{c}{H}.$$

So as time tends to infinity, the light signal penetrates a comoving distance of only $R_1 r = \sqrt{3/\Lambda}$. Objects beyond a comoving distance of $\sqrt{3/\Lambda}$ cannot be seen, because the intervening space is expanding so quickly that even a light signal cannot cross it. But H is constant and the expansion rate is unchanging, so this is true at *any* time. What this would look like is a fixed horizon around you at a distance of $\sqrt{3/\Lambda}$, and neighbouring galaxies being accelerated away from you towards this horizon and out of your observable Universe, which is gradually being emptied out. However, you would never see a galaxy *cross* this horizon: its redshift would get larger as it approached the horizon, and if you could watch a clock in that galaxy, the time dilation of that clock would get longer. If t_2 is the coordinate time when the galaxy reaches the horizon, then you would see the clock slow at it approached t_2, but it would never quite reach t_2 from your point of view. However, from the galaxy's point of view, the passage of time is unaffected. There, they would see *your* clocks running slowly, as you passed out of *their* observable Universe.

You may recognize this redshifting and time dilation from descriptions of objects falling into the event horizon of a black hole (which you will also meet in Chapter 6). Indeed, the horizon at $\sqrt{3/\Lambda}$ is a **cosmological event horizon**. The Universe in the far future will look like a black hole, but inside-out.

Exercise 1.7 How big, in megaparsecs and in metres, will the cosmological event horizon be? You will need the cosmological parameters in Section 1.5. How does this compare to the current size of the observable Universe? ■

How far ahead can we look? When Ralph Alpher and George Gamow realized that the early Universe was hot and dense enough for nuclear reactions, and calculated the amount of heavy elements production, they were condemned by some physicists for their rashness. What grounds do we have, the critics argued, for believing that the same physical theories applied three minutes after the Big Bang? The Universe provided the rebuttal: the predictions of primordial nucleosynthesis have been very extensively confirmed, as we shall see in later chapters. Nevertheless, the words of warning from these critics should still ring in our ears as we extrapolate to the distant future.

At the moment all the baryons in the Universe are either involved in the cycle of star birth and death, or could potentially take part. However, by about the year one trillion (10^{12} years), the Universe will be too sparse to support more star

formation. At that point, baryons will either be in degenerate matter (in white dwarfs or neutron stars), or be locked up in brown dwarfs, or have fallen into black holes, or just be atoms or molecules too sparsely distributed to form new stars. Looking further ahead, we eventually reach the epoch of possible proton decay.

In the standard model of particle physics, the proton is stable and does not decay. However, some 'grand unified theories' in particle physics predict eventual proton decay. The best current limit on proton half-life $t_{1/2}$ comes from the Super-Kamiokande experiment in Japan, which found $t_{1/2} > 10^{35}$ years. Perhaps 10^{35} years is the furthest ahead that one might venture to predict the contents of the Universe. But who would be around to contradict you if you got it wrong?

Summary of Chapter 1

1. In a flat Euclidean space, the number counts of a homogeneous and isotropic distribution of objects vary as $\mathrm{d}N/\mathrm{d}S \propto S^{-5/2}$, but the total flux diverges.
2. In special relativity, lengths and times are not observer-independent, but the relativistic interval s is invariant.
3. $\delta s = 0$ always for light rays, and $\delta s = c\,\delta\tau$ always for massive particles, where τ is proper time.
4. Any homogeneous, isotropic expanding Universe consistent with special relativity can be described by the Robertson–Walker metric

$$\mathrm{d}s^2 = c^2\,\mathrm{d}t^2 - R^2(t)\left(\frac{\mathrm{d}r^2}{1-kr^2} + r^2\,\mathrm{d}\theta^2 + r^2\sin^2\theta\,\mathrm{d}\phi^2\right). \quad \text{(Eqn 1.6)}$$

5. Cosmological redshift z, given by

$$1 + z = \frac{R_0}{R_1} = \frac{1}{a} = \frac{\lambda_{\text{observed}}}{\lambda_{\text{emitted}}}, \quad \text{(Eqn 1.10)}$$

   is caused by the expansion of the Universe, not by the Doppler effect. Random galaxy motions (known as proper motions) can contribute additional red or blue shifts from the relativistic Doppler effect.
6. Nevertheless, if one regards cosmological redshift as an *apparent* recession velocity, then the apparent velocity is proportional to distance from the observer, with the constant of proportionality known as the Hubble parameter.
7. The contributions to the energy density of the Universe from matter and the cosmological constant are denoted as Ω_{m} and Ω_Λ, respectively, and are defined by

$$\Omega_{\mathrm{m}} = \frac{8\pi G\rho_{\mathrm{m}}}{3H^2}, \quad \text{(Eqn 1.15)}$$

$$\Omega_\Lambda = \frac{\Lambda c^2}{3H^2}. \quad \text{(Eqn 1.17)}$$

   These determine the age and fate of the Universe.
8. Neglecting radiation, if $\Omega_{\mathrm{m}} + \Omega_\Lambda = 1$ at any time, then this is true at all times. Also, if either Ω_{m} or Ω_Λ is zero, then this is also true at all times. In all other situations, there is a fine-tuning problem in the early Universe for the values of Ω_{m} and Ω_Λ.

9. 'Distance' can have several meanings in a Robertson–Walker metric. We have defined the angular diameter distance, proper motion distance and luminosity distance:

$$d_{\mathrm{A}} = \frac{D}{\theta}, \qquad \text{(Eqn 1.47)}$$

$$d_{\mathrm{M}} = \frac{u}{\mathrm{d}\theta/\mathrm{d}t}, \qquad \text{(Eqn 1.48)}$$

$$d_{\mathrm{L}} = \left(\frac{L}{4\pi S}\right)^{1/2}. \qquad \text{(Eqn 1.49)}$$

   These give different but related values for the distance. Angular diameter distance has a maximum value, so objects placed further away could sometimes appear larger.

10. The comoving distance to any distant object is the current proper distance, neglecting peculiar velocities. (This turns out to be equal to the proper motion distance when $k = 0$.)
11. The proper size of the observable Universe is increasing at a rate much larger than the speed of light, c. An object moving in a flat spacetime is a very different physical situation to free-floating objects in an expanding space.
12. The currently-accepted cosmological parameters imply that the foreseeable fate of the Universe is exponential expansion.

Further reading

- For a more leisurely introduction to the Robertson–Walker metric, see Lambourne, R., 2010, *Relativity, Gravitation and Cosmology*, Cambridge University Press.
- For a useful review of distance measures in cosmology (though pre-dating dark energy, which we shall meet in later chapters, and the observation that $\Omega_\Lambda \simeq 0.7$), see Carroll, S.M., Press, W.H. and Turner, E.L., 1992, 'The cosmological constant', *Annual Review of Astronomy and Astrophysics*, **30**, 499.

Acknowledgements

Grateful acknowledgement is made to the following sources:

Figures

Cover image courtesy of the Spitzer Space Telescope, ©NASA/JPL-Caltech/STScI/CXC/UofA/ESA/AURA/JHU;

Figure 1.9: supernova data taken from Blondin, S. et al. (2008) *The Astrophysical Journal*, **682**, 724; Figure 1.10 top left: http://astrosurf.com, Christian Buil; Figure 1.10 top right: European Southern Observatory (ESO); Figure 1.10 bottom left: Stanford, S. A. et al. (2000) 'The first sample of ultraluminous infrared galaxies at high redshift', *The Astrophysical Journal Supplement Series*, **131**, 185, The American Astronomical Society; Figure 1.10 bottom right: van Dokkum, P. G. et al. (2005) 'Gemini near-infrared spectrograph observations of a red star-forming galaxy at $z = 2.225$: evidence of shock ionization due to a galactic wind', *The Astrophysical Journal*, **622**, L13, The American Astronomical Society; Figure 1.11: Carroll, S. M. (2004), 'Why is the Universe accelerating?', Freedman, W. L. ed. Measuring and Modelling the Universe, Carnegie Observatories Astrophysics Series, **2**, Carnegie Observatories; Figure 1.13: NASA and the Hubble Heritage Team (STScI/AURA); Figure 1.16: Springel, V. et al. (2005) 'Simulations of the formation, evolution and clustering of galaxies and quasars', *Nature*, **435**, 629 ; Figures 1.18 & 1.19: adapted from Carroll, S. M., Press, W. H. and Turner, E. L. (1992) 'The Cosmological Constant', *Annual Review of Astronomy & Astrophysics*, **30**, 499, ©Annual Reviews Inc.; Figure 1.20: Adapted from Knop R. A. et al. (2003), 'New Constraints on Ω_{M}, Ω_{Λ} and w from an independent set of 11 high-redshift supernovae observed with the Hubble Space Telescope', *The Astrophysical Journal*, **598**, 102, ©The American Astronomical Society;

Figures 2.1, 2.2 & 2.9: NASA/WMAP Science Team; Figure 2.3: adapted from Coc, A. (2009) 'Big-bang nucleosynthesis: a probe of the early Universe', *Nuclear Instruments & Methods in Physics Research A*, **611**, 224, Elsevier Science BV; Figure 2.4: adapted from a figure by Professor Edward L. Wright, UCLA; Figures 2.7 & 2.8: Peacock, J. A. (1999) *Cosmological Physics*, Cambridge University Press; Figure 2.10: University of Hawaii; Figure 2.11: Granett, B. R. et al. (2008) 'An imprint of super-structures on the microwave background due to the Integrated Sachs–Wolfe effect', *The Astrophysical Journal Letters*, **683**, L99, Institute of Physics Publishing; Figure 2.12: adapted from Dunkley, J. et al. (2009) 'Five year Wilkinson Microwave Anisotropy Probe (WMAP1) observations: likelihoods and parameters from the WMAP data', *Astrophysical Journal Supplement Series*, **180**, 306, Institute of Physics Publishing; Figures 2.13 & 2.15: Hu, W. and Dodelson, S. (2002) 'Cosmic microwave background anisotropies', *Annual Reviews of Astronomy & Astrophysics*, **40**, 171, Annual Reviews; Figures 2.14 & 3.7: adapted from figures by Edward L. Wright, UCLA and based on data from Kowalski, M. et al. (2009) *The Astrophysical Journal Supplement Series*, **686**, 749; Figure 2.16: adapted from Larson, D. et al. (2010) 'Seven year Wilkinson Microwave Anisotropy Probe (WMAP1) observations: power spectra and WMAP-derived parameters', *Astrophysical Journal Supplement Series* (in press, arXiv:1001.4635), Institute of Physics Publishing; Figures 2.17 & 2.18: adapted from Komatsu, E. et al. (2009)

'Five year Wilkinson Microwave Anisotropy Probe (WMAP1) Observations: cosmological interpretation' *Astrophysical Journal Supplement Series*, **180**, 330, Institute of Physics Publishing;

Figure 3.1a: Justin Yaros and Andy Schlei/Flynn Haase/NOAO/AURA/NSF; Figure 3.1b: adapted from Begeman, K. G., Broeils, A. H. and Sanders, R. H. (1991) 'Extended rotation curves of spiral galaxies: dark haloes and modified dynamics', *Monthly Notices of the Royal Astronomical Society*, **249**, 523; Figure 3.2: ESO Online Digital Sky Survey www.eso.org/dss/dss.; Figure 3.4: adapted from a figure of Professor Edward L. Wright, UCLA; Figure 3.5: adapted from Dressler, A. (1980) 'Galaxy morphology in rich clusters: implications for the formation and evolution of galaxies', *The Astrophysical Journal*, **236**, 351, American Astronomical Society; Figure 3.6: adapted from Ciardullo, R. (2004) 'The Planetary Nebula Luminosity Function', A contribution to the ESO International Workshop on *Planetary Nebulae beyond the Milky Way*, Garching (Germany), May 19–21, 2004; Figure 3.8: Chris Schur, www.schursastrophotography.com; Figure 3.9: www.astro.uu.se; Figure 3.10: NASA/Jason Ware; Figure 3.11: Günter Kerschhuber, Gahberg Observatory; Figures 3.12 & 3.13: Richard Powell, www.atlasoftheuniverse.com; Figure 3.14: adapted from de Lapparent, V. et al. (1986) 'A slice of the Universe', *The Astrophysical Journal*, **302**, 1, The American Astronomical Society; Figures 3.15 & 3.18: The 2dF Galaxy Redshift Survey team (http://www2.aao.gov.au/2dFGRS/); Figure 3.16: adapted from Peacock, J. A. et al. (2001) 'A measurement of the cosmological mass density from clustering in the 2dF Galaxy Redshift Survey', *Nature*, **410**, 169, Nature Publishing Group; Figure 3.17: adapted from Peacock, J. A. and Dodds, S. J. (1994), 'Reconstructing the linear power spectrum of cosmological mass fluctuations', *Monthly Notices of the Royal Astronomical Society*, **267**, 1020, The Royal Astronomical Society; Figure 3.19: adapted from Percival, W. J. et al. (2007) 'Measuring the Baryon Acoustic Oscillation Scale using the Sloan Digital Sky Survey and 2df Galaxy Redshift Survey', *Monthly Notices of the Royal Astronomical Society*, **381**, 1053, The Royal Astronomical Society;

Figure 4.1: adapted from Tegmark, M. and Zaldarriaga, M. (2002) 'Separating the Early Universe from the Late Universe: cosmological parameter estimation beyond the black box', *Physical Review D*, **66**(10), 103508, The American Physical Society; Figure 4.2: adapted from Lacey, C. and Cole, S. (1993) 'Merger rates in hierarchical models of galaxy formation', *Monthly Notices of the Royal Astronomical Society*, **262**, 627, The Royal Astronomical Society; Figure 4.5: Moore, B. et al. (1999) 'Dark matter substructure within galactic halos', *The Astrophysical Journal*, **524**, L19, American Astronomical Society; Figure 4.6: adapted from Rocca-Volmerange, B. and Guiderdoni, B. (1988) 'An atlas of synthetic spectra of galaxies', *Astronomy & Astrophysics Supplement Series*, **75**, 93, European Southern Observatory; Figure 4.7: Dr Henner Busemann, School of Earth, Atmospheric and Environmental Sciences (SEAES), The University of Manchester; Figure 4.8: adapted from Gordon, K. D. et al. (2003) 'A quantitative comparison of the Small Magellanic Cloud, Large Magellanic Cloud, and Milky Way ultraviolet to near-infrared extinction curves', *The Astrophysical Journal*, **594**, 279, The American Astronomical Society; Figure 4.9: Brammer, G. B. et al. (2008) 'EAZY: A fast, public photometric redshift code', *The Astrophysical Journal*, **686**, 1503, The American Astronomical Society; Figure 4.10: adapted

from Dey, A. et al. (1998) 'A galaxy at $z = 5.34$', *The Astrophysical Journal*, **498**, L93, The American Astronomical Society; Figure 4.11: adapted from Bell, E. F. et al. (2003) 'The optical and near infrared properties of galaxies. 1. luminosity and stellar mass functions', *The Astrophysical Journal Supplement Series*, **149**, 289, The American Astronomical Society; Figure 4.12: NRAO; Figure 4.13: Sloan Digital Sky Survey; Figure 4.14: adapted from Yates, M. G. and Garden R. P. (1989) 'Near-simultaneous optical and infrared spectrophotometry of active galaxies', *Monthly Notices of the Royal Astronomical Society*, **241**, 167, The Royal Astronomical Society; Figure 4.16: adapted from Figure 2.3 of Peterson, B. M. (1997) *An Introduction to Active Galactic Nuclei*, Cambridge University Press; Figure 4.17: adapted from Richards, G. T. et al. (2006), 'The Sloan Digital Sky Survey Quasar Survey: quasar luminosity function from data release 3', *The Astronomical Journal*, **131**, 2766, The American Astronomical Society; Figure 4.18 left: A. Fujii; Figure 4.18 right: R. Williams (STScI), the Hubble Deep Field Team and NASA; Figure 4.19: Robert Williams and the Hubble Deep Field Team (STScI) and NASA; Figure 4.20: NASA/ESA, CXC, JPL-Caltech, STScI, NAOJ, J. E. Greach (Univ Durham) et al.; Figure 4.21: adapted from Gabasch, A. et al. (2004) 'The evolution of the luminosity functions in the FORS deep field from low to high redshift', *Astronomy & Astrophysics*, **421**, 41, ESO; Figure 4.22: NASA, ESA, S. Beckwith (STScI) and the HUDF Team; Figures 4.23 & 4.24: adapted from Bouwens, R. J. et al. (2009) 'Constraints on the first galaxies: z 10 Galaxy Candidates from HST WFC3/IR', Submitted to Nature (arXiv:0912.4263); Figure 4.25: adapted from Cohen, J. G. et al. (1996) 'Redshift clustering in the Hubble Deep Field', *The Astrophysical Journal*, **471**, 5, The American Astronomical Society; Figure 4.26: adapted from Bouwens, R. J. et al. (2004) 'Galaxy size evolution at high redshift and surface brightness selection effects:constraints from the Hubble Ultra Deep Field', *The Astrophysical Journal*, **611**, 1. The American Astronomical Society; Figure 4.27: adapted from van Dokkum, P. G., Kriek, M. and Franx, M. (2009) 'A high stellar velocity dispersion for a compact massive galaxy at redshift $z = 2.186$', *Nature* , **460**, 717, Macmillan Publishers Limited; Figure 4.28: NASA Jet Propulsion Laboratory (NASA-JPL); Figure 4.29: H. Ferguson, M. Dickinson, R. Williams, STScI and NASA; Figure 4.30: adapted from Bell, E. F. et al. (2004) 'Nearly 5000 distant early type galaxies in COMBO-17: a red sequence and its evolution since z 1', *The Astrophysical Journal*, **608**, 752, The American Astronomical Society;

Figure 5.1: adapted from Hauser, M. G. and Dwek, E. (2001) 'The Cosmic Infrared Background: Measurements and Implications', *Annual Review of Astronomy & Astrophysics*, **39**, 249, Annual Reviews Inc; Figure 5.2: adapted from Hopwood, R. H. et al. 'Ultra deep AKARI observations of Abell 2218: resolving the 15 m extragalactic background light', *Astrophysical Journal Letters*, **716**, 45; Figure 5.3: http://alma.asiaa.sinica.edu.tw; Figure 5.4: adapted from Blain, A. W. et al. (2002) 'Submillimeter galaxies', *Physics Reports*, **369**, 111, Elsevier Science B.V.; Figure 5.5: adapted from Hughes D. H. et al. (1998) 'High-redshift star formation in the Hubble Deep Field revealed by a submillimetre-wavelength survey', *Nature*, **394**, 241; Figure 5.6: BLAST Collaboration; Figure 5.7: ESA and SPIRE Consortium; Figure 5.8: adapted from Serjeant, S. et al. (1998) 'A spectroscopic study of IRAS F10214+4724', *Monthly Notices of the Royal Astronomical Society*, **298**, 321, Royal Astronomical Society; Figure 5.9: adapted from Surace, J. A. et al. (1998) 'HST/WFPC2 Observations

of warm ultraluminous infrared galaxies', *Astrophysical Journal*, **492**, 116, The American Astronomical Society; Figure 5.10 top: Brad Whitmore (STScI) and NASA; Figure 5.10 bottom: NASA/JPL-Caltech/Z. Wang (Harvard-Smithsonian CfA); Visible: M. Rushing/NOAO; Figure 5.11: Courtesy of JAXA; Figures 5.12 & 5.13: adapted from Condon, J. J. (1992) 'Radio emission from normal galaxies', *Annual Reviews of Astronomy & Astrophysics*, **30**, 575, Annual Reviews Inc; Figure 5.14: adapted from Dole, H. et al. (2006) 'The cosmic infrared background resolved by Spitzer', *Astronomy & Astrophysics*, **451**, 417, EDP Sciences; Figures 5.15 & S5.1: adapted from Griffin, M. et al. (2007) 'The Herschel-SPIRE instrument and its capabilities for extragalactic astronomy', *Advances in Space Research*, **40**, 612, ©COSPAR, Published by Elsevier Ltd; Figures 5.16, 5.17 & 5.18: Pérez-González, P. G. et al. (2008) 'The Stellar Mass Assembly of Galaxies from $z = 0$ to $z = 4$', *The Astrophysical Journal*, **675**, 234, The American Astronomical Society; Figure 5.19: adapted from Le Floc'h, E. et al. (2005) 'Infrared Luminosity Functions from the Chandra Deep Field-South', *The Astrophysical Journal*, **632**, 169, The American Astronomical Society; Figure 5.20: adapted from Di Matteo, T. et al. (2005) 'Energy input from quasars regulates the growth and activity of black holes and their host galaxies', *Nature*, **433**, 604, Nature Publishing Group; Figure 5.21: McNamara, B. R. et al. (2000) 'Chandra X-ray observations of the Hydra A cluster:an interaction between the radio source and the X-ray emitting gas', *Astrophysical Journal*, **534**, L135, The American Astronomical Society; Figures 5.22 & 5.23: Fabian, A. C. et al. (2003) 'A very deep Chandra observation of the Perseus cluster: shocks and ripples', *Monthly Notices of the Royal Astronomical Society*, **344**, L43, The Royal Astronomical Society;

Figure 6.3: Science Photo Library; Figure 6.4: Misner, C. W., Thorne, K. S. and Wheeler, J. A. (1973) *Gravitation*, W. H. Freeman & Co Ltd; Figure 6.5: adapted from Kormendy, J. (1988) 'Evidence for a supermassive black hole in the nucleus of M31', *The Astrophysical Journal*, **325**, 128, American Astronomical Society; Figure 6.6: adapted from Miyoshi, M. et al. (1995) 'Evidence for a black hole from high rotation velocities in a sub parsec region of NGC4258', *Nature*, **373**, 127, Nature Publishing Group; Figure 6.7: adapted from Schdel, R. et al. (2003) 'Stellar dynamics in the central arcsecond of our galaxy', *The Astrophysical Journal*, **596**, 1015, The American Astronomical Society; Figures 6.8 & 6.9: adapted from Peterson, B. M. (2001) 'Variability of active galactic nuclei', Aretxaga, I., Knuth, D. and Mujica, R. eds. Advanced Lectures on the Starburst-AGN Connection, World Scientific; Figure 6.10: Ferraresse, L. (2002) 'Black Hole Demographics', Proceedings of the 2nd KIAS Astrophysics Workshop held in Seoul, Korea (Sep 3–7 2001), Lee, C. H. ed. World Scientific; Figure 6.11: J. Schmitt et al. ROSAT Mission, MPE, ESA; Figure 6.13: Brandt, W. N. and Hasinger, G. (2005) 'Deep Extragalactic X-ray Surveys', *Annual Review of Astronomy & Astrophysics*, **43**, 827, Annual Reviews; Figure 6.14: X-ray: NASA/CXC/U. of Michigan/J. Liu et al.; Optical: NOAO/AURA/NSF/T. Boroson; Figure 6.15: adapted from Alexander, D. M. et al. (2008) 'Weighing the black holes in $z \approx 2$ submillimeter-emitting galaxies hosting active galactic nuclei', *The Astrophysical Journal*, **135**, 1968, The American Astronomical Society; Figure 6.16: adapted from Kauffmann, G. and Heckman, T. M. (2009) 'Feast and famine: regulation of black hole growth in low redshift galaxies', *Monthly Notices of the Royal Astronomical Society*, **397**, 135,

The Royal Astronomical Society; Figure 6.17: Weisberg, J. M. and Taylor, J. H. (2005) 'The relativistic binary pulsar B1913+16: thirty years of observations ad analysis', Rasio, F. A. and Stairs, I. H. (eds) Binary Radio Pulsars, *ASP Conference Series*, **328**, 25, Astronomical Society of the Pacific; Figure 6.18: CalTech; Figure 6.19: adapted from Boroson, T. A. and Lauer, T. R. (2009) 'A candidate sub-parsec supermassive binary black hole system', *Nature*, **458**, 53, Nature Publishing Group;

Figure 7.3: NASA, Andrew Fruchter and the ERO Team [Sylvia Baggett (STScI), Richard Hook (ST-ECF), Zoltan Levay (STScI)] (STScI); Figure 7.4: adapted from Nguyen, H. T. et al. (1999) 'Hubble Space Telescope imaging polarimetry of the gravitational lens FSC 10214+4724', *The Astronomical Journal*, **117**, 671, The American Astronomical Society; Figure 7.5: adapted from Serjeant, S. et al. (1998) 'A spectroscopic study of IRAS F10214+4724', *Monthly Notices of The Royal Astronomical Society*, **298**, 321, The Royal Astronomical Society; Figure 7.12: Dr A. Holloway, University of Manchester; Figure 7.17: Burke, B. et al. (1993) *Sub-Arcsecond Radio Astronomy*, Davis, R. J. and Booth, R. S. eds. Cambridge University Press; Figure 7.18: adapted from Alcock, A. et al. (1993) 'Possible gravitational microlensing of a star in the Large Magellanic Cloud', *Nature*, **365**, 621, Nature Publishing Group; Figure 7.20: Stephane Colombi, International Astronomical Union; Figure 7.22: adapted from Blandford, R. D. et al. (1991) 'The distortion of distant galaxy images by large scale structure', *Monthly Notices of the Royal Astronomical Society*, **251**, 600, The Royal Astronomical Society; Figure 7.23: adapted from Hoekstra, H. et al. (2004) 'Properties of galaxy dark matter halos from weak lensing', *The Astrophysical Journal*, **606**, 67, The American Astronomical Society; Figures 7.24 & 7.25: adapted from Massey, R. et al. (2007) 'Dark matter maps cosmic scaffolding', *Nature*, **445**, 286, Nature Publishing Group; Figure 7.26: Large Synoptic Survey Telescope Corporation; Figure 7.27: top right panel adapted from Hopwood et al. (2010) *Astrophysical Journal Letters*, **716**, 45; bottom left panel adapted from Egami et al., paper in preparation; Figure 7.28: X-ray: NASA/CXC/CfA/ M. Markevitch et al. Lensing Map: NASA/STScI; ESO WFI; Magellan/U. Arizona/D. Clowe et al. Optical: NASA/STScI; Magellan/U. Arizona/D. Clowe et al.; Figure 7.29: CASTLES (CfA-Arizona Space Telescope Lens Survey); Figure 7.30: NASA Johnson Space Center Collection; Figure 7.31: A. Bolton (UH IfA) for SLACS and NASA/ESA; Figure S7.1: NASA, ESA, C. Faure (Zentrum für Astronomie, University of Heidelberg) and J. P. Kneib (Laboratoire d'Astrophysique de Marseille);

Figure 8.1: Rauch, M. (1998) 'The Lyman alpha forest in the spectra of quasistellar objects', *Annual Reviews of Astronomy & Astrophysics*, **36**, 267, Annual Reviews; Figure 8.4: NASA, ESA, Y. Izotov (Main Astronomical Observatory, Kyiv, UA) and T. Thuan (University of Virginia); Figures 8.5, 8.6 & 8.7: Pettini, M. et al. (2008) 'Deuterium abundance in the most metal-poor damped Lyman alpha system', *Monthly Notices of the Royal Astronomical Society*, **391**, 1499, The Royal Astronomical Society; Figure 8.8 adapted from Kriss, G. A. et al. (1999) 'The Ultraviolet Peak of the Energy Distribution in 3C 273: Evidence for an Accretion Disk and Hot Corona around a Massive Black Hole', *The Astrophysical Journal*, **527**, 683, The American Astronomical Society; Figures 8.9 & 8.14: adapted from Noterdaeme, P. et al. (2009) 'Evolution of the cosmological mass density of neutral gas from Sloan

Digital Sky Survey II-data release 7', *Astronomy & Astrophysics*, **505**, 1087, European Southern Observatory; Figure 8.10: Prochaska, J. X. et al. (2005) 'The SDSS damped Ly alpha survey: data release 3', *Astrophysical Journal*, **635**, 123, The American Astronomical Society; Figure 8.12: Reynolds, S. C. (2007) 'Quasar Absorbers and the InterGalactic Medium', taken from a pedagogical Seminar at the Royal Observatory, Edinburgh, 8 March 2007, www.roe.ac.uk/ifa/postgrad/pedagogy/2007_reynolds.pdf; Figure 8.13: Möller, P. and Warren, S. J. (1993) 'Emission from a damped Ly alpha absorber at $z = 2.81$', *Astronomy & Astrophysics*, **270**, 43, European Southern Observatory; Figure 8.15: Smette, A. et al. (1992) 'A spectroscopic study of UM 673 A & B: on the size of the Lyman-alpha clouds', *Astrophysical Journal*, **389**, 39, The American Astronomical Society; Figure 8.16: Nick Gnedin, Department of Astronomy & Astrophysics, The University of Chicago; Figures 8.17 & 8.19: Fan, X. et al. (2006) 'Observational constraints on cosmic reionization', *Annual Review of Astronomy & Astrophysics*, **44**, 415 ©2006 by Annual Reviews; Figure 8.18: Becker, G. D. et al. (2007) The evolution of optical depth in the Ly alpha Forest: evidence against reionization at z 6, *The Astrophysical Journal*, **662**, 72, The American Astronomical Society; Figure 8.20: adapted from Möller, P. and Jakobsen, P. (1990) 'The Lyman continuum opacity at high redshifts: through the Lyman forest and beyond the Lyman valley', *Astronomy & Astrophysics*, **228**, 299, European Southern Observatory; Figure 8.21: Smette, A. et al. (2002) 'Hubble Space Telescope Space Telescope Imaging System Observations of the He II Gunn–Peterson effect toward HE 2347-4342', *Astrophysical Journal*, **564**, 542, The American Astronomical Society; Figure 8.23: Carilli, C. L. et al. (2002) 'H I 21 centimeter absorption beyond the epoch of reionization', *The Astrophysical Journal*, **577**, 22, The American Astronomical Society; Figures 8.24 & 8.25: Cristiani, S. et al. (2007) 'The CODEX-ESPRESSO experiment: cosmic dynamics, fundamental physics, planets and much more . . .', *Il Nuovo Cimento*, **122B**, 1165, Societa Italiana di Fisica.

Every effort has been made to contact copyright holders. If any have been inadvertently overlooked the publishers will be pleased to make the necessary arrangements at the first opportunity.